Acute avoidance of hydrogen sulfide is modulated by external and internal states in *C. elegans*

Longjun Pu[1, 2, 3], Lina Zhao[1, 2, 3], Jing Wang[1, 2, 3], Johan Henriksson[1, 4, 5], Patrick Laurent[6], Changchun Chen[1, 2, 3*]

[1]Department of Molecular Biology, Umeå University, Umeå, Sweden

[2]Umeå Centre for Molecular Medicine, Umeå University, Umeå, Sweden

[3]Wallenberg Centre for Molecular Medicine, Umeå University, Umeå, Sweden

[4]The Laboratory for Molecular Infection Medicine Sweden (MIMS), Umeå University, Umeå, Sweden

[5]Integrated Science Lab (Icelab), Umeå University, Umeå, Sweden

[6]Laboratory of Neurophysiology, ULB Neuroscience Institute (UNI), Université Libre de Bruxelles (ULB), Belgium

*Corresponding author

E-mail: changchun.chen@umu.se

Abstract

Hydrogen sulfide (H_2S) can act as an energy source, a poison and a gasotransmitter in organisms. We used the robust locomotory responses to H_2S in *Caenorhabditis elegans* to delineate the molecular mechanisms governing sensory and adaptive responses to H_2S exposure. We found that *C. elegans* exhibited transiently increased locomotory activity and turning behavior as a strategy to escape the noxious H_2S stimulation. The behavioral responses to H_2S were modulated by a complex network of signaling pathways, including cyclic GMP signaling in ciliated sensory neurons, calcineurin, nuclear hormone receptors, to the major starvation regulators such as insulin and TGF-β signaling. The response to H_2S was substantially affected by the ambient O_2 levels and their prior experience in low O_2 environments, suggesting an intricate interplay between O_2 and H_2S sensing mechanisms. Prolonged exposure to H_2S robustly evoked H_2S detoxification coupled with reduced locomotory response to the subsequent H_2S challenges. Intriguingly, the expression of genes involved in iron homeostasis, including *ftn-1* and *smf-3*, was substantially modified in exposure to H_2S, implying that labile iron levels are affected by H_2S. In support of this, iron supplement significantly bolstered the behavioral response to H_2S. In addition, mitochondria, one of the central hubs for H_2S metabolism, played a crucial role in adaptive responses to H_2S. In summary, our study provides molecular insights into the mechanisms through which *C. elegans* detects, modulates, and adapts its response to H_2S.

Introduction

The detection and response to chemical signals are crucial to interact effectively with the environment in various organisms, spanning from bacteria to humans. During the late Proterozoic era, the rise in oxygen (O_2) levels eliminated hydrogen sulfide (H_2S) from most of the habitats. Yet, low O_2 levels together with high concentrations of H_2S and carbon dioxide (CO_2) can still persist in enclosed environments where bacteria actively decompose organic matter (Olson & Straub, 2016). H_2S can easily penetrate biological membranes and interfere with various cellular processes, leading to toxicity. One of its detrimental effects is the disruption of cellular respiration by binding to cytochrome c oxidase (COX) and inhibiting the mitochondrial electron transport chain (Cooper & Brown, 2008; Khan et al., 1990; Nicholls & Kim, 1982b).

Animals inhabiting environments rich in H_2S have evolved mechanisms to either avoid or adapt to high concentrations of H_2S, providing them with survival advantages. Species that encounter periodic increases in H_2S often possess sensing abilities and exhibit avoidance behaviors. For example, benthic species undertake daily vertical migrations between sulfidic and non-sulfidic waters (Abel, Koenig, & Davis, 1987; Salvanes, Utne-Palm, Currie, & Braithwaite, 2011). Certain metazoan species have seized the ecological opportunities presented by H_2S-rich environments through the development of cellular adaptations, allowing them to occupy a unique ecological niche that is inaccessible to the other organisms. Livebearing fish species, for instance, have evolved COX subunits that are more resistant to H_2S and are more efficient in H_2S detoxification (Kelley et al., 2016; Pfenninger et al., 2014).

Free living nematodes thrive in decaying matter where they are exposed to significant fluctuations in O_2, CO_2, and H_2S levels over short distances (Rodriguez-Kabana, Jordan, & Hollis, 1965). Nematodes like *C. elegans* have evolved the ability to utilize these gasous stimuli to navigate their environment, locate bacterial food sources, or escape the dangers (Bretscher, Busch, & de Bono, 2008; Carrillo, Guillermin, Rengarajan, Okubo, & Hallem, 2013). Acute exposure to H_2S triggers transiently increased locomotion in *C. elegans* (Budde

67 & Roth, 2011). However, prolonged exposure to H_2S induces cellular adaptation to survive
68 the toxic environment. *C. elegans* can tolerate H_2S levels up to 50 ppm, but the concentrations
69 exceeding 150 ppm prove lethal (Budde & Roth, 2010, 2011; Fawcett, Hoyt, Johnson, &
70 Miller, 2015; Horsman, Heinis, & Miller, 2019; Miller, Budde, & Roth, 2011a; Miller &
71 Roth, 2007). Extended periods of low O_2 and/or high H_2S exposure stabilize the hypoxia-
72 inducible factor HIF-1, leading to transcriptional reprogramming (Budde & Roth, 2010).
73 Through HIF-1-dependent and independent mechanisms, acclimation of *C. elegans* to 50 ppm
74 H_2S extends lifespan and improves the response to hypoxia-induced protein aggregation
75 (Budde & Roth, 2010; Fawcett et al., 2015; Horsman et al., 2019; Miller & Roth, 2007;
76 Qabazard et al., 2014).
77 In this study, we investigated how the nematode *C. elegans* responds acutely to avoid
78 an increase of H_2S levels, as well as how it adapts at the molecular and physiological levels if
79 they fail to escape the H_2S exposure.
80
81 **Results**
82 **cGMP signaling in ASJ cilia contributes to H_2S avoidance**
83 When encountering aversive cues such as noxious gases, *C. elegans* initiates a pirouette
84 followed by an increase of its locomotory activity to escape the noxious stimuli. When
85 acutely exposed to 150 ppm H_2S, *C. elegans* exhibited an increased locomotory speed and
86 enhanced turning behavior, while decreasing the frequency of reversals, as a strategy to
87 escape the noxious stimuli (***Figure 1—figure supplement 1A–C***). The maximum speed was
88 reached after 6–8 minutes in H_2S, and returned to the baseline over a period of approximately
89 1 hour (***Figure 1—figure supplement 1D***). The reduced locomotory activity after 2 hours in
90 H_2S was fully reversible if these animals were immediately challenged by a different stimulus
91 such as hypoxia (***Figure 1—figure supplement 1E***). The magnitude of the avoidance
92 responses appeared to be concentration dependent. Under our assay conditions, acute

93 behavioral response to 50 ppm H_2S was minimal and lacked consistency, whereas the
94 response to 150 ppm H_2S was robust and reproducible (***Figure 1—figure supplement 1F***).
95 To gain molecular insight into H_2S evoked locomotory response, we performed a
96 candidate screen for mutants that failed to increase their locomotory speed when H_2S levels
97 acutely increased to 150 ppm (***Supplementary file 1***). We discovered that mutants defective
98 in ciliogenesis exhibited diminished H_2S responses (***Figure 1A–C***). These included *daf-19*
99 mutants lacking cilia, *dyf-3* mutants with reduced cilia length, and *dyf-7* mutants where
100 ciliogenesis occurs but the cilia are not anchored to their sensilla and are not exposed to the
101 external environment (Heiman & Shaham, 2009; Murayama, Toh, Ohshima, & Koga, 2005;
102 Starich et al., 1995; Swoboda, Adler, & Thomas, 2000). Our observations suggest that cilia
103 exposure to the external environment is necessary for H_2S detection. Cilia-mediated sensory
104 responses often involve the activation of guanylate cyclases and the opening of cGMP-gated
105 channels (Ferkey, Sengupta, & L'Etoile, 2021). We observed attenuated H_2S responses in *tax-*
106 *4* or *tax-2* mutants, lacking the key subunits of cilia-enriched cGMP-gated channels (***Figure***
107 ***1D and E***). Comparable observations have also been reported in acute response to CO_2,
108 suggesting that locomotory responses to CO_2 and H_2S are similar (Bretscher et al., 2008;
109 Hallem et al., 2011; Hallem & Sternberg, 2008). Consistent with this, mutations in genes
110 encoding the calcineurin subunits TAX-6 or CNB-1, or nuclear hormone receptor NHR-49,
111 impaired both H_2S and CO_2 responses (Hallem & Sternberg, 2008) (***Figure 1—figure***
112 ***supplement 2A–C***). Additionally, locomotory response to H_2S was also repressed following a
113 24-hour period of starvation, as observed for CO_2 (***Figure 1—figure supplement 2D***)
114 (Bretscher et al., 2008; Hallem & Sternberg, 2008). In *C. elegans*, the regulation of
115 starvation-responses involves the reduced activity of two major pathways: insulin and TGF-β
116 signaling. Disrupting the genes encoding the insulin receptor DAF-2 or the TGF-β ligand
117 DAF-7 eliminated locomotory activity in response to acute H_2S (***Figure 1F and G, Figure***
118 ***1—figure supplement 2E***). Insulin and TGF-β signaling involve the inhibition of
119 downstream transcription factors DAF-16 or DAF-3 respectively. H_2S avoidance defects of

120 *daf-2* and *daf-7* mutants were fully suppressed in *daf-2; daf-16* or in *daf-7; daf-3* double
121 mutants (***Figure 1F and G***).
122 These observations prompted us to further investigate if the same molecular and
123 circuit mechanisms underlay the acute avoidance to CO_2 and H_2S. The response to CO_2
124 requires receptor guanylate cyclase GCY-9 (Hallem et al., 2011). Interestingly, GCY-9 was
125 dispensable for the locomotory responses to H_2S (***Figure 1H***). In addition, animals responded
126 more rapidly to CO_2 than to H_2S, but with a reduced magnitude (***Figure 1I***), implying that
127 distinct mechanisms likely drive these two responses. In a comprehensive survey of all
128 guanylate cyclase mutants, the *daf-11* strain emerged as the only mutant showing defects in
129 the avoidance of H_2S (***Figure 1D, Supplementary file 1***). Selective expression of *daf-11* in
130 ASJ neurons, but not in other neurons, partially restored the locomotory response to acute
131 H_2S (***Figures 1J, Figure 1—figure supplement 2F–I***). Consistently, the H_2S response defect
132 of *tax-4* mutants was also rescued by selective expression of its cDNA in ASJ neurons
133 (***Figure 1K***), suggesting that the receptor guanylate cyclase DAF-11 and the CNG channel
134 TAX-4 partially act in ASJ neurons to promote acute response to H_2S. This differed from the
135 site of action of the CO_2 sensor GCY-9, which primarily operates in BAG neurons (Hallem et
136 al., 2011). Taken together, these observations suggest that common signaling pathways
137 modulate the locomotory responses to both H_2S and CO_2, although the molecular and circuit
138 underpinning of H_2S and CO_2 sensing are different.
139
140 **Activation of the O_2 sensing circuit antagonizes H_2S avoidance**
141 The sensory responses of wild *C. elegans* are adapted to their living environment, which is
142 characterized by low O_2 levels and high concentrations of CO_2. In comparison to the
143 domesticated lab strain N2, wild isolates of *C. elegans* exhibit a strong response to high O_2
144 but are relatively indifferent to CO_2 (Beets et al., 2020; Bretscher et al., 2008; Hallem &
145 Sternberg, 2008). Local H_2S concentrations could also be significantly higher in decomposing
146 substances where wild *C. elegans* thrives. We suspected that wild strains could display a
147 modified response to H_2S in comparison to standard laboratory N2 animals. Indeed, wild

148 isolates CB4855, CB4856, and CB4858 exhibited attenuated responses to H_2S (***Figure 2A,***
149 ***Figure 2—figure supplement 1A***). One predominant genetic trait in these strains is a
150 naturally occurring variation of neuropeptide receptor NPR-1 215F, which is less active than
151 NPR-1 215V in N2 animals (de Bono & Bargmann, 1998). This led us to investigate whether
152 the NPR-1 signaling plays a role in modulating acute avoidance of H_2S. Mutating *npr-1* in N2
153 strain background was sufficient to abolish locomotory responses to H_2S, as observed in the
154 wild isolates (***Figure 2B***). NPR-1 primarily acts within the RMG interneurons to modulate
155 responses to environmental stimuli by reducing signal output from these neurons (Laurent et
156 al., 2015; Macosko et al., 2009). The selective expression of the highly active *npr-1(215V)*
157 variant in RMG neurons effectively restored H_2S evoked locomotory response in *npr-1*
158 mutant worms (***Figure 2C***). Furthermore, optogenetic stimulation of RMG interneurons using
159 channelrhodopsin-2 (ChR2) significantly dampened locomotory response to H_2S of N2
160 animals, suggesting high RMG activity inhibits H_2S responses (***Figure 2—figure supplement***
161 ***1B***).
162 The sensation of 21% O_2 involves the soluble guanylate cyclases GCY-35/GCY-36
163 and the downstream cyclic nucleotide gated (CNG) channels TAX-4/TAX-2 (Busch et al.,
164 2012; Cheung, Cohen, Rogers, Albayram, & de Bono, 2005; Couto, Oda, Nikolaev, Soltesz,
165 & de Bono, 2013; Gray et al., 2004; Laurent et al., 2015; Persson et al., 2009; Zimmer et al.,
166 2009). We examined if disrupting O_2 sensing machinery had the same effect as the inhibition
167 of RMG signaling by NPR-1(215V). We found that silencing O_2 sensing neurons by mutating
168 *gcy-35* and *tax-4*, or ablating these neurons by cell-specific expression of the pro-apoptotic
169 gene *egl-1* restored H_2S evoked behavioral response in *npr-1* null mutants (***Figure 2D–F***).
170 Specific expression of *gcy-35* cDNA in URX, AQR, PQR was sufficient to repress acute
171 response to H_2S in *npr-1; gcy-35* double mutants (***Figure 2G***). Finally, enhancing the
172 presynaptic activities of URX, AQR, PQR neurons by the expression of a gain-of-function
173 PKC-1(A160E) (Dekker, Mcintyre, & Parker, 1993; Hiroki et al., 2022) significantly
174 dampened H_2S regulated locomotory activity (***Figure 2—figure supplement 1C***). Taken

175 together, these observations indicate that activation of O_2 sensing circuit is inhibitory to H_2S
176 evoked locomotory response.
177
178 **H_2S exposure reprograms gene expression in *C. elegans***
179 Prolonged exposure to H_2S has a dramatic impact on the physiology of *C. elegans*: 50 ppm
180 H_2S exposure extends its lifespan, while 150 ppm H_2S is lethal (Budde & Roth, 2010, 2011;
181 Fawcett et al., 2015; Horsman et al., 2019; Miller & Roth, 2007 Miller, 2011 #5). We
182 conducted a comparative analysis of the transcriptome profiles in animals exposed to either
183 50 ppm or 150 ppm H_2S for the durations of 1 hour, 2 hours, or 12 hours. Our RNA-seq
184 analysis revealed that a one-hour exposure to either 50 ppm or 150 ppm H_2S was sufficient to
185 trigger significant changes in gene expression, with 518 or 304 genes showing differential
186 expression, respectively (***Figure 3A, Supplementary file 2, p<1e-10***). Genes induced by 1-
187 hour and 2-hour H_2S exposure displayed a considerable overlap (***Figure 3B, Figure 3—***
188 ***figure supplement 1A***). Gene Ontology (GO) analysis revealed that biological processes such
189 as defense against bacteria and cysteine biosynthesis from L-serine were immediately
190 activated upon H_2S exposure (***Figure 3C and D, Figure 3—figure supplement 1B and C***).
191 As expected, we observed a robust induction of genes involved in H_2S detoxification (***Figure***
192 ***3E and F***) (Miller, Budde, & Roth, 2011b; Niu et al., 2011; Vora et al., 2022). H_2S is
193 detoxified in mitochondria by sulfide:quinone oxidoreductase SQRD-1 to persulfide, which is
194 then metabolized by sulfur dioxygenase ETHE-1 to generate sulfite. Thiosulfate transferase
195 further oxidizes sulfite to produce thiosulfate (Hildebrandt & Grieshaber, 2008). Glutathione
196 S-transferases (GSTs) remove accumulated sulfur molecules during H_2S oxidation (Jackson,
197 Melideo, & Jorns, 2012). Notably, *gst-19* and *sqrd-1* were among the most significantly
198 upregulated genes after one or two hours of exposure to either 50 ppm or 150 ppm H_2S, while
199 *ethe-1* showed a weak increase (***Figure 3E and F, Figure 3—figure supplement 1D and E,***
200 ***Supplementary file 2***). H_2S activates the HIF-1 pathway through the interaction of
201 sulhydrylase/cysteine synthase CYSL-1 with the HIF-1 proline hydroxylase EGL-9 (Ma,

202 Vozdek, Bhatla, & Horvitz, 2012). We found that a proportion of genes with HIF-1 regulated
203 promoters displayed increased expression after 1 or 2 hours of H_2S exposure (***Figure 3—***
204 ***figure supplement 1F***) (Miller et al., 2011b; Vora et al., 2022). These genes included the
205 above-mentioned detoxifying enzymes GST-19, SQRD-1, and ETHE-1, as well as enzymes
206 involved in cysteine metabolism, CYSL-1, CYSL-2, and CDO-1 (***Supplementary file 2***).
207 Mutations increasing SKN-1 activity bypass the requirement for HIF-1 to survive in high H_2S
208 (Horsman et al., 2019). Consistent with early observations (Miller et al., 2011a), we also
209 observed that a set of SKN-1 targets were differentially expressed in H_2S (***Figure 3—figure***
210 ***supplement 1G***) (Niu et al., 2011). This included the heat shock protein encoding genes *hsp-*
211 *16.2* and *hsp-16.41* (***Figure 3E and F, Figure 3—figure supplement 1D and E***).
212 Surprisingly, we also observed a rapid increase in the expression of genes associated with
213 intracellular H_2S production, such as *semo-1* and *mpst-3* genes (***Figure 3E and F, Figure***
214 ***3—figure supplement 1D and E***) (Philipp et al., 2022; Qabazard et al., 2014). However,
215 these data aligned with earlier observations made in sulfide spring fish (Kelley et al., 2016;
216 Mathew, Schlipalius, & Ebert, 2011; Qabazard et al., 2014).
217 When exposed to the H_2S for 12 hours, the differentially expressed genes showed
218 reduced overlap with those identified at earlier time points (***Figure 3B, Figure 3—figure***
219 ***supplement 1A***). This suggests that different defense strategies against H_2S might be
220 employed at various stages of exposure. Although similar sets of genes were induced after 1h
221 or 2h at 50 ppm and 150 ppm H_2S, the overlap between 50ppm and 150ppm decreased after
222 12 hours exposure (***Figure 3—figure supplement 1H–J***). This observation suggests that
223 defense mechanisms might also differ for prolonged exposure at low and high levels of H_2S.
224 In particular, we noted that 150 ppm H_2S specifically triggered the expression of the HIF-1
225 regulator *rhy-1* and the HIF-1 target *nhr-57* at all exposure time points, which was less
226 pronounced in response to 50 ppm H_2S (***Figures 3E and F, Figure 3—figure supplement***
227 ***1D, E, K and L***).
228

229 **Acute response to H_2S is modulated by HIF-1 signaling**

230 Consistent with early observations (Budde & Roth, 2010), our RNA-seq data suggested that
231 H_2S exposure activates HIF-1 pathway (***Figure 3—figure supplement 1F***). Stabilization of
232 HIF-1 by H_2S is critical for animals to survive H_2S exposure by the induction of
233 detoxification genes as well as other adaptative responses (Ma et al., 2012). Such an
234 adaptation is usually accompanied with the reduction in sensory sensitivity to this stressor.
235 Therefore, we suspected that HIF-1 stabilization might dampen the acute response to H_2S.
236 Under normoxia conditions, the conserved proline-4-hydroxylase PHD/EGL-9 hydroxylates
237 HIF-1, which is subsequently recognized by the von Hippel-Lindau (VHL) tumor suppressor
238 protein for degradation (Kaelin & Ratcliffe, 2008; Semenza, 2010). We found that disrupting
239 *hif-1* resulted in extremely transient behavioral response to H_2S characterized by an initial
240 bout of activity and a rapid decline of locomotory speed to the basal level (***Figure 4A***). While
241 eliminating PHD/EGL-9 or VHL activity, which stabilizes HIF-1, the locomotory response to
242 H_2S was completely inhibited (***Figure 4B***). *egl-9; hif-1* or *vhl-1; hif-1* double mutants had the
243 identical response as *hif-1* mutants (***Figure 4C and D***), confirming that mutating *egl-9* or *vhl-*
244 *1* inhibits acute response to H_2S by activating HIF-1. Acclimating animals in 1% O_2 for more
245 than 12 hours also significantly decreased acute response to H_2S (***Figure 4E***). In addition,
246 animals carrying the non-degradable form of HIF-1 in all neurons were defective in H_2S
247 evoked locomotory responses (***Figure 4F***). Taken together, these observations suggest that
248 constitutive activation of HIF-1 promotes the adaption to H_2S and inhibits the behavioral
249 responses to H_2S stimulation.

250 The transient behavioral response to H_2S in *hif-1* mutants suggested that animals
251 deficient of HIF-1 can still detect the presence of H_2S. This observation together with the
252 importance of HIF-1 signaling in H_2S detoxification provoked us to explore whether
253 detoxification enzymes were also required for the sustained locomotory activity in H_2S.
254 Similar to *hif-1* mutants, both *sqrd-1* and *ethe-1* mutants displayed a transient response to H_2S
255 (***Figure 4G and H***). We next examined the contribution of other upregulated genes in
256 response to H_2S, including the genes encoding sulfhydrylase/cysteine synthases CYSL-1,

257 CYSL-2, and CYSL-3 as well as SEMO-1. Disrupting CYSLs and SEMO-1 encoding genes
258 phenocopied *hif-1* or *sqrd-1* mutants (***Figure 4I and J***). Our data suggest that while H_2S
259 detoxification system is not essential for H_2S sensing, it is required for preserving animals'
260 locomotory activity in the presence of H_2S.
261
262 **Labile iron pool is critical to sustain the locomotory activity in H_2S**
263 *C. elegans* tightly regulates iron homeostasis through the control of iron transporter SMF-3,
264 as well as the regulation of iron storage protein Ferritins FTN-1 and FTN-2 (Cha'on et al.,
265 2007; Gourley, Parker, Jones, Zumbrennen, & Leibold, 2003; Kim, Cho, Yoo, & Ahnn, 2004;
266 Pekec et al., 2022). Among the most differentially regulated genes, *ftn-1* appeared to be
267 consistently downregulated by H_2S (***Figure 5A and B, Figure 5—figure supplement 1A–D***).
268 The inhibited expression of *ftn-1* and *ftn-2* as well as the elevated expression of *smf-3* (***Figure***
269 ***5A and B, Figure 5—figure supplement 1A–D***) prompted us to explore if labile iron levels
270 play a role in behavioral response to H_2S exposure. The labile iron pool is chelatable and
271 redox-active. In the presence of iron chelator 2,2'-dipyridyl (BP), H_2S evoked locomotory
272 response was fully inhibited (***Figure 5C***). This was not caused by the general sickness of BP-
273 exposed animals as they responded robustly to acute hypoxia (***Figure 5—figure supplement***
274 ***1E***). By contrast, the supplementation of ferric ammonium citrate (FAC) significantly
275 prolonged animals' locomotory activity in H_2S (***Figure 5C***). In addition, disrupting *ftn-1*,
276 which was expected to increase labile iron levels (Anderson & Leibold, 2014; Romney,
277 Newman, Thacker, & Leibold, 2011), promoted the locomotory activity of animals in H_2S
278 (***Figure 5D***), Conversely, mutating *smf-3*, which impaired iron uptake (Anderson & Leibold,
279 2014; Romney et al., 2011), led to a faster decline of locomotory activity in H_2S (***Figure 5D***).
280 Furthermore, depleting labile iron pool by *ftn-1* overexpression resulted in an attenuated
281 response to H_2S (***Figure 5E***), while it did not affect acute response to hypoxia (***Figure 5—***
282 ***figure supplement 1F***). These data suggests that high levels of free iron sustain locomotory
283 activity in H_2S, whereas low iron levels inhibit behavioral responses to H_2S. It has been

284 reported that hypoxia inhibits the expression of *ftn-1* and *ftn-2*, while upregulating *smf-3*
285 expression (Ackerman & Gems, 2012; Gourley et al., 2003; Romney et al., 2011).
286 Additionally, *hif-1* mutants have been reported to display reduced intracellular iron content
287 and increased susceptibility to iron starvation (Rajan et al., 2019; Romney et al., 2011). We
288 explored if the locomotory defect of *hif-1* mutants in H_2S could be explained by iron
289 deficiency (Rajan et al., 2019; Romney et al., 2011). The presence of FAC significantly
290 improved H_2S evoked locomotory activity of *hif-1* mutants (***Figure 5F***). In addition,
291 disrupting *ftn-1* partially suppressed the locomotory defect of *hif-1* mutants in H_2S (***Figure***
292 ***5G***). These data confirm that labile iron pool is critical to maintain the locomotory activity of
293 animals in H_2S.
294 Iron deficiency causes mitochondrial dysfunction including decreased cytochrome
295 concentration and respiratory efficiency (Dallman, 1986; Masini, Salvioli, et al., 1994;
296 Masini, Trenti, et al., 1994; Walter et al., 2002). H_2S is known to exert both positive and
297 negative effects on the mitochondria, which are not only the primary targets of H_2S but also
298 represent one of the main cellular hubs of H_2S detoxification (Cooper & Brown, 2008; Khan
299 et al., 1990; Nicholls & Kim, 1982a). We probed the possibility that impairing mitochondrial
300 function might alter locomotory response to H_2S. To this end, we tested mutants with the
301 disruption of *gas-1*, *clk-1*, *mev-1,* or *isp-1* genes. Similar to iron depletion, these mutants
302 abrogated locomotory response to H_2S (***Figure 6A–D***). Additionally, exposing animals to the
303 mitochondrial complex I inhibitor rotenone fully repressed locomotory response to H_2S
304 (***Figure 6E***). While rotenone exposure inhibits H_2S response, it evoked increased locomotory
305 activity over 2 hours (***Figure 6E***). These observations confirm the critical role of
306 mitochondria in supporting locomotory response in exposure to H_2S in *C. elegans*.
307
308 **Discussion**
309 Animals' behavior and physiology are profoundly influenced by the surrounding
310 environment, in which they reside. Wild *C. elegans* isolates thrive in the decomposing
311 matters, where the local concentrations of O_2 are low while the levels of CO_2 and H_2S could

312 be high. These animals have adapted their behavior in such an environment, displaying
313 increased sensitivity to high O_2 exposure but dampened responses to CO_2. In contrast, the
314 standard laboratory strain N2, which is constantly exposed to high O_2 but low CO_2, is
315 relatively insensitive to elevated levels of O_2 but robustly avoids CO_2 exposure (Beets et al.,
316 2020; Bretscher et al., 2008; Carrillo et al., 2013; Hallem & Sternberg, 2008). As observed in
317 response to CO_2, N2 animals exhibit strong reorientation and acceleration to escape the H_2S
318 exposure, while wild isolates display a significantly diminished response to H_2S.
319 The responses to CO_2 and H_2S in N2 animals are modulated by common signaling
320 pathways, which include the ciliogenesis, the cGMP-gated channels TAX-2 and TAX-4,
321 calcineurin subunit TAX-6/CNB-1, and nuclear hormone receptor NHR-49. Additionally,
322 these two responses are affected by the nutritional state of the animals. In *C. elegans*,
323 starvation is signaled by reduced activity in two major signaling pathways: the insulin and
324 TGF-β pathways. H_2S and CO_2 responses are abolished in starved animals or mutants that
325 disrupt insulin or TGF-β signaling. Therefore, the modulation of behavioral responses to H_2S
326 and CO_2 by external and internal factors appears highly similar. However, CO_2 response is
327 mediated by the guanylate cyclase GCY-9 in BAG neurons (Hallem et al., 2011), which
328 appears to be dispensable for H_2S sensing. We observed a prominent role for the guanylate
329 cyclase DAF-11 expressed in the chemosensory neurons ASJ for H_2S responses. *daf-11*
330 signaling in ASJ also mediates chemosensory responses to volatile chemicals and to NO
331 (Birnby et al., 2000; Hao et al., 2018). However, DAF-11 controls the normal larval
332 development of *C. elegans* and may have pleiotropic indirect effects on sensory functions
333 (Murakami, Koga, & Ohshima, 2001). In absence of more direct evidence, its role as H_2S
334 sensor in ASJ remain uncertain.
335 Long-term exposure to H_2S can elicit adaptive responses including changes in gene
336 expression patterns to mitigate the toxic effects of H_2S. Within just one hour of H_2S exposure,
337 we observed the upregulation of genes associated with H_2S detoxification. This response
338 enables animals to detoxify H_2S and maintain cellular homeostasis under sulfidic conditions.
339 This adaptive strategy is accompanied by the reduced locomotory response to H_2S exposure.

340 The HIF-1 (hypoxia-inducible factor) signaling is a major pathway involved in the adaption
341 during prolonged H_2S exposure (Budde & Roth, 2011; Miller et al., 2011b). When the HIF-1
342 pathway is constitutively induced in the nervous system, the behavioral responses to H_2S are
343 eliminated. Similarly, reduced behavioral responses to H_2S are observed after 12 hours of
344 exposure to 1% O_2. It has been proposed that persulfides, polysulfides, and thiosulfate, which
345 are the by-products during sulfide detoxification, play a role in H_2S signaling (Mishanina,
346 Libiad, & Banerjee, 2015). However, in the case of locomotion responses to H_2S in *C.*
347 *elegans*, this is unlikely to be the mechanism for the initial response, as mutants lacking
348 detoxification enzymes still exhibit an acute and transient response to H_2S. Interestingly, the
349 sustained locomotory activity was abolished in these mutants, suggesting that either the by-
350 products of H_2S detoxification contribute to maintain the behavioral response or the lack of
351 detoxification enzyme results in rapid cellular toxicity, preventing sustained locomotory
352 activity in H_2S (Budde & Roth, 2011).

353 Interestingly, we provide evidence that labile iron pool is critical for H_2S responses.
354 Removal of labile iron pool by the chelator BP or *ftn-1* overexpression attenuated both acute
355 and sustained responses to H_2S, suggesting that intracellular iron is required for the sensation
356 of H_2S. While increasing labile iron levels sustains the locomotory activity in H_2S. In *C.*
357 *elegans*, labile iron homeostasis is predominantly regulated by the HIF-1 signaling, the
358 activation of which decreases the transcription of *ftn-1* and increases the expression of *smf-3*
359 (Ackerman & Gems, 2012; Romney et al., 2011). Consistent with this, we have observed a
360 downregulation of the ferritins FTN-1 and FTN-2, as well as an upregulation of the iron
361 transporter SMF-3 during exposure to H_2S. This suggests that H_2S may control the expression
362 of FTN-1 and SMF-3, and consequently the labile iron pool, through the HIF-1 pathway.

363 Although the exact mechanisms are not yet fully understood, several possibilities
364 shed light on the importance of labile iron for H_2S responses. Fe^{2+} acts as a critical cofactor
365 for the PHD/EGL-9 enzymes, which are involved in the hydroxylation-dependent
366 destabilization of HIF-1 (Myllyharju & Kivirikko, 1997). PHD inactivation by iron
367 sequestration by ferritin can increase HIF-1 signaling, suggesting a potential role of labile

368 iron as a negative feedback loop to limit HIF-1 activity (Siegert et al., 2015). In addition, iron
369 is necessary for the biosynthesis of iron-sulfur (Fe-S) clusters, critical cofactors involved in
370 redox reactions and mitochondrial respiration (Read, Bentley, Archer, & Dunham-Snary,
371 2021; Xu & Moller, 2011). Labile iron is beneficial for the biogenesis of Fe-S clusters despite
372 its oxidative properties under normal O_2 conditions (Liochev, 1996). Interestingly, hypoxia
373 has been observed to enhance Fe-S cluster biogenesis by increasing the availability of
374 bioactive iron (Ast et al., 2019). Therefore, low oxidative stress may alleviate the need to
375 maintain a low labile iron pool. In this context, the antioxidant properties of H_2S or the
376 interruption of mitochondrial respiration by H_2S might provide condition favorable to high
377 labile iron pool (Shefa, Kim, Jeong, & Jung, 2018; Sunda, Kieber, Kiene, & Huntsman,
378 2002).

379 The primary mechanism underlying the toxic effects of H_2S has been suggested to be
380 the direct inhibition of cytochrome c oxidase, a critical enzyme involved in mitochondrial
381 respiration (Cooper & Brown, 2008; Khan et al., 1990; Nicholls & Kim, 1982b). Intriguingly,
382 we have observed that genetic and pharmacological inhibition of mitochondrial respiration
383 prevents the locomotory response of *C. elegans* to H_2S. This effect may be mediated by the
384 induction of the HIF-1 pathway, which has been observed in mutants with impaired
385 mitochondrial respiration (Lee, Hwang, & Kenyon, 2010). Furthermore, acute inhibition of
386 mitochondrial respiration by rotenone also enhances locomotion while suppressing the
387 response to H_2S. Reducing mitochondrial respiration has been found to stimulate aversive
388 behavior in *C. elegans* (Melo & Ruvkun, 2012). Therefore, the acute inhibition of
389 mitochondrial respiration by H_2S could transiently promote aversive behavior in *C. elegans*,
390 while long-term inhibition of mitochondrial respiration may contribute to the induction of the
391 HIF-1 pathway and adaptation to H_2S.

392 In summary, this study unveils a novel behavior of *C. elegans* in their avoidance to
393 H_2S. The response to H_2S is intricately shaped by their environment, where it integrates with
394 other sensory signals, including food availability, CO_2 and O_2 levels. We emphasize the vital
395 role of H_2S detoxification system, particularly the involvement of mitochondria and labile

396 irons, in sustaining the locomotory activity in H_2S. In the future, it will be exciting to
397 elucidate the neuronal mechanisms driving H_2S avoidance and to explore how the changes of
398 labile iron pools modulate cellular and organismal behavior responses to noxious sensory
399 stimuli.
400
401 **Materials and Methods**
402 **Strains**
403 *C. elegans* were maintained using standard protocols (Brenner, 1974). Strains used in this
404 study are listed in ***Supplementary file 1*** and ***Supplementary file 3***.
405
406 **Preparation of H_2S gas mixture**
407 Different H_2S concentrations were created as previously described (Miller & Roth, 2007).
408 Briefly, the H_2S-containing gas mixture were prepared by diluting 5000 ppm H_2S in nitrogen
409 (N_2) with 7% O_2 balanced with N_2. The gas flow was tuned by Sierra Smart-Trak 100 mass
410 flow controllers. H_2S concentration in the mixture was measured using two H_2S detectors
411 (MSA ALTAIR 2X gas detector for H_2S and Clip Single Gas Detector, SDG, CROWCON).
412 The pre-defined gas mixtures of 7% O_2, 1% O_2 and 5% CO_2 with N_2 were purchased from Air
413 Liquide Gas AB. 5000 ppm H_2S stock in N_2 was obtained from Linde Gas AB. Gas mixtures
414 in all experiments were hydrated before use.
415
416 **Molecular Biology**
417 The Multisite Gateway system (Thermo Fisher Scientific, United States) was used to generate
418 expression vectors. Promoters, including *gcy-37* (2.7kb), *trx-1* (1 kb), *ftn-1*(2 kb), *daf-11*(3
419 kb), *odr-3*(2.7 kb), *gpa-11*(3 kb), *sra-6*(3 kb), *odr-1*(2.4 kb), *flp-21*(4.1kb), and *ocr-2*(2.4 kb)
420 were amplified from N2 genomic DNA and cloned into pDONR P4P1 using BP clonase. g*cy-*
421 *35*, *tax-4* and *pkc-1* cDNAs were amplified using the first strand cDNA library as the
422 template, while *daf-11* and *ftn-1* genomic sequences were amplified using genomic DNA as
423 the template. The entry clones of these genes pDONR 221 were generated using BP reaction.

424 To generate the gain of function mutation of *pkc-1* (A160E), Q5 Site-Directed Mutagenesis
425 Kit (NEB) was used according to manufacturer instructions. All expression vectors were
426 generated using LR reaction. The primer sequences were displayed in ***Supplementary file 4***.
427 To generate transgenic animals, the *daf-11* expression vectors were injected at the
428 concentration of 20 ng/µl supplemented with 50 ng/µl of a coelomocyte co-injection marker
429 (*unc-122p::GFP)* and 30 ng/µl of 1kb DNA ladder. For *tax-4* gene, the injection mixtures
430 were prepared using 40 ng/µl of *tax-4* expression vectors, 50 ng/µl of a coelomocyte co-
431 injection marker and 10 ng/µl of 1kb DNA ladder. The rest of expression constructs were
432 injected at 50 ng/µl together with 50 ng/µl of a coelomocyte marker.
433
434 **CRISPR/Cas9 genome editing**
435 Genes were disrupted using CRISPR/Cas-9 mediated genome editing as described (Dokshin,
436 Ghanta, Piscopo, & Mello, 2018; Ghanta & Mello, 2020). The strategy involved the
437 utilization of homology-directed insertion of custom designed single strand DNA template
438 (ssODN), which had two homology arms of 35bp flanking the targeted PAM site. Between
439 two homology arms, a short sequence containing a unique restriction enzyme cutting site and
440 in frame as well as out of frame stop codons was included. The insertion of ssODN template
441 would delete 16 bases of coding sequence, ensuring the proper gene disruption. To prepare
442 the injection cocktail, 0.5 µl of Cas-9 protein (IDT) was mixed with 5 µl of 0.4µg/µl
443 tracrRNA (IDT, United States) and 2.8 µl of 0.4 µg/µl crRNA (IDT). The mixture was
444 incubated at 37°C for at least 10 minutes before 2.2 µl of 1µg/µl ssODN (or 500 ng dsDNA)
445 and 2 µl of 0.6 µg/µl *rol-6* co-injection marker were added. Nuclease-free water was used to
446 bring the final volume to 20 µl. The injection mixture was centrifuged for 2 minutes before
447 use.
448
449 **Behavioral assays**
450 H_2S evoked locomotion activity was monitored as described previously (Laurent et al., 2015;
451 Zhao et al., 2022). Briefly, OP50 bacteria were seeded on the assay plates 16 hours before

452 use. The border of bacterial lawn was removed using a PDMS stamp. For each assay, 25 to 30
453 day-one adult animals were picked onto assay plates, allowed to settle down for 15 minutes,
454 and subsequently sealed within microfluidic chambers. A syringe pump (PHD 2000, Harvard
455 Apparatus) was employed to deliver gas mixtures into the microfluidic chamber at a constant
456 flow of 3 ml/min. The rapid switch between different gas mixtures were controlled by Telfon
457 valves coupled with ValveBank Perfusion Controller (AutoMate Scientific). The locomotory
458 activity at different gas mixtures were monitored using a high-resolution camera (FLIR)
459 mounted on a Zeiss Stemi 508 microscope. Videos were captured at a rate of 2 frames per
460 second, starting with a 2-minute recording in 7% O_2, followed by 11 minutes in H_2S, and
461 ending with a final 5-minute period in 7% O_2. For the long-term recording in H_2S, video
462 capture commenced with a 2-minute period in 7% O_2, followed by a duration of 148 minutes
463 in 150 ppm H_2S, and concluded with a final 2-minute interval in 7% O_2.

464 To assess the effects of rotenone on H_2S evoked locomotory response, day-one adult
465 animals were subjected to 10 μM rotenone for 10min, 30min, 1 hour and 2 hours on the drug
466 containing plates. Subsequently, the rotenone-treated animals were assayed on the standard
467 assay plates without the drug. To explore the impact of ferric ammonium citrate (FAC)
468 (F5879, Sigma-Aldrich) and 2,2′-Bipyridyl (BP) (D216305, Sigma-Aldrich) on behavioral
469 response to H_2S, L4 animals were exposed to 100 μM FAC or 5mg/ml BP for 16 hours in the
470 presence of bacterial food. The FAC or BP treated animals were assayed on FAC or BP
471 containing plates.

472 Optogenetic experiments were performed as previously outlined (Zhao et al., 2022).
473 Transgenic L4 animals were exposed to 100μM all-trans retinal (ATR) (R2500, Sigma) in the
474 dark for 16 hours. The ATR-fed animals were assayed with the illumination of 70 $\mu W/mm^2$
475 blue light during the whole assay period. Blue light was emitted from an ultra-high-power
476 LED lamp (UHP-MIC-LED-460, Prizmatix), and the light intensity was determined using a
477 PM50 Optical Power Meter (ThorLabs). To minimize the effect of transmitted light on the
478 transgenic animals, a long-pass optical filter was used to eliminate the lights with short
479 wavelengths during picking. All videos of behavioral analysis were analyzed using a home-

480 made MATLAB program Zentracker (https://github.com/wormtracker/zentracker). For all
481 behavior analyses, at least three assays were performed for each strain with more than 80
482 worms in total.
483
484 **RNA extraction and sequencing**
485 To obtain RNA samples for RNA-seq, thirty young adult animals were picked to each fresh
486 plate and allowed to lay eggs for 2 hours, after which the adult animals were removed and
487 eggs were allowed to develop into day one adults. Day one animals were subsequently
488 challenged with H_2S for three different time points (1 hour, 2 hours and 12 hours). For each
489 time point, five plates of day one animals were exposed to 50 ppm H_2S, 150 ppm H_2S or 7%
490 O_2 as a control group. Subsequently, the animals were immediately collected and rinsed three
491 times with M9 buffer. After washing, the worm pellet was frozen in liquid nitrogen. Animals
492 were homogenized using Bullet Blender (Next Advance) in the presence of Qiazol Lysis
493 Reagent and 0.5mm Zirconia beads at 4°C. RNA was prepared using RNeasy Plus Universal
494 Mini Kit (Qiagen). Six independent RNA samples were prepared for all different treatments.
495 The 2100 Bioanalyzer instrument (Agilent) was used for the RNA quality control with a
496 microfluidic chip specific for RNA (Agilent RNA 6000 Nano Kit). Then 1 μg of qualified
497 RNA samples in RNase-free ddH2O was used for library preparation. Library was
498 constructed and sequenced by Novogene.
499
500 **RNA-seq analysis**
501 The RNA-seq data was aligned using STAR v2.7.9a (Dobin et al., 2013) and gene expression
502 counts extracted by featureCounts v2.0.3 (Liao, Smyth, & Shi, 2014). Differential expression
503 was calculated using DESeq2 (Love, Huber, & Anders, 2014). GO analysis was performed
504 using the EnrichR R package (Kuleshov et al., 2016) on genes having p.adj < 1e-10. For
505 brevity, several highly similar GO categories were manually omitted (full EnrichR output
506 available at Github repository).
507

508 **Data availability**

509 Raw sequencing data has been deposited at ArrayExpress # E-MTAB-13296. The R code is

510 available at https://github.com/henriksson-lab/ce_h2s_tc.

511

512 **Acknowledgments**

513 We thank the Caenorhabditis Genetics Center (funded by NIH Office of Research

514 Infrastructure Programs P40 OD010440) and the National BioResources Project Japan for

515 strains.

516

517 **Funding**

518 The computations were enabled by resources provided by the National Academic

519 Infrastructure for Supercomputing in Sweden (NAISS) and the Swedish National

520 Infrastructure for Computing (SNIC) at UPPMAX partially funded by the Swedish Research

521 Council through grant agreements no. 2022-06725 and no. 2018-05973. This work is

522 supported by the Swedish VR Research Council grant MIMS (2021-06602) to J.H., the

523 Belgian National Fund for Scientific Research (FRS-FNRS) to P.L., the ERC starting grant

524 (802653 OXYGEN SENSING), the Swedish Research Council VR starting grant (2018-

525 02216), and the Wallenberg Centre for Molecular Medicine (Umeå) to C.C.

526

527 **References**

528 Abel, D. C., Koenig, C. C., & Davis, W. P. (1987). Emersion in the Mangrove Forest Fish

529 Rivulus-Marmoratus - a Unique Response to Hydrogen-Sulfide. *Environmental*

530 *Biology of Fishes, 18*(1), 67-72. doi:Doi 10.1007/Bf00002329

531 Ackerman, D., & Gems, D. (2012). Insulin/IGF-1 and Hypoxia Signaling Act in Concert to

532 Regulate Iron Homeostasis in *Caenorhabditis elegans*. *Plos Genetics, 8*(3).

533 doi:ARTN e1002498

534 10.1371/journal.pgen.1002498

Anderson, C. P., & Leibold, E. A. (2014). Mechanisms of iron metabolism in *Caenorhabditis elegans*. *Frontiers in Pharmacology, 5*. doi:ARTN 113 10.3389/fphar.2014.00113

Ast, T., Meisel, J. D., Patra, S., Wang, H., Grange, R. M. H., Kim, S. H., . . . Mootha, V. K. (2019). Hypoxia Rescues Frataxin Loss by Restoring Iron Sulfur Cluster Biogenesis. *Cell, 177*(6), 1507-+. doi:10.1016/j.cell.2019.03.045

Beets, I., Zhang, G., Fenk, L. A., Chen, C., Nelson, G. M., Felix, M. A., & de Bono, M. (2020). Natural Variation in a Dendritic Scaffold Protein Remodels Experience-Dependent Plasticity by Altering Neuropeptide Expression. *Neuron, 105*(1), 106-121 e110. doi:10.1016/j.neuron.2019.10.001

Birnby, D. A., Link, E. M., Vowels, J. J., Tian, H., Colacurcio, P. L., & Thomas, J. H. (2000). A transmembrane guanylyl cyclase (DAF-11) and Hsp90 (DAF-21) regulate a common set of chemosensory behaviors in *Caenorhabditis elegans*. *Genetics, 155*(1), 85-104. Retrieved from <Go to ISI>://WOS:000086869200008

Brenner, S. (1974). The genetics of *Caenorhabditis elegans*. *Genetics, 77*(1), 71-94. doi:10.1093/genetics/77.1.71

Bretscher, A. J., Busch, K. E., & de Bono, M. (2008). A carbon dioxide avoidance behavior is integrated with responses to ambient oxygen and food in *Caenorhabditis elegans*. *Proc Natl Acad Sci U S A, 105*(23), 8044-8049. doi:10.1073/pnas.0707607105

Budde, M. W., & Roth, M. B. (2010). Hydrogen sulfide increases hypoxia-inducible factor-1 activity independently of von Hippel-Lindau tumor suppressor-1 in *C. elegans*. *Mol Biol Cell, 21*(1), 212-217. doi:10.1091/mbc.E09-03-0199

Budde, M. W., & Roth, M. B. (2011). The response of *Caenorhabditis elegans* to hydrogen sulfide and hydrogen cyanide. *Genetics, 189*(2), 521-532. doi:10.1534/genetics.111.129841

Busch, K. E., Laurent, P., Soltesz, Z., Murphy, R. J., Faivre, O., Hedwig, B., . . . de Bono, M. (2012). Tonic signaling from O(2) sensors sets neural circuit activity and behavioral state. *Nat Neurosci, 15*(4), 581-591. doi:10.1038/nn.3061

563 Carrillo, M. A., Guillermin, M. L., Rengarajan, S., Okubo, R. P., & Hallem, E. A. (2013). O-
564 2-Sensing Neurons Control CO2 Response in *C. elegans*. *Journal of Neuroscience,*
565 *33*(23), 9675-9683. doi:10.1523/Jneurosci.4541-12.2013
566 Cha'on, U., Valmas, N., Collins, P. J., Reilly, P. E., Hammock, B. D., & Ebert, P. R. (2007).
567 Disruption of iron homeostasis increases phosphine toxicity in *Caenorhabditis*
568 *elegans*. *Toxicol Sci, 96*(1), 194-201. doi:10.1093/toxsci/kfl187
569 Cheung, B. H., Cohen, M., Rogers, C., Albayram, O., & de Bono, M. (2005). Experience-
570 dependent modulation of *C. elegans* behavior by ambient oxygen. *Curr Biol, 15*(10),
571 905-917. doi:10.1016/j.cub.2005.04.017
572 Cooper, C. E., & Brown, G. C. (2008). The inhibition of mitochondrial cytochrome oxidase
573 by the gases carbon monoxide, nitric oxide, hydrogen cyanide and hydrogen sulfide:
574 chemical mechanism and physiological significance. *J Bioenerg Biomembr, 40*(5),
575 533-539. doi:10.1007/s10863-008-9166-6
576 Couto, A., Oda, S., Nikolaev, V. O., Soltesz, Z., & de Bono, M. (2013). In vivo genetic
577 dissection of O2-evoked cGMP dynamics in a *Caenorhabditis elegans* gas sensor.
578 *Proc Natl Acad Sci U S A, 110*(35), E3301-3310. doi:10.1073/pnas.1217428110
579 Dallman, P. R. (1986). Biochemical Basis for the Manifestations of Iron-Deficiency. *Annual*
580 *Review of Nutrition, 6*, 13-40. doi:DOI 10.1146/annurev.nu.06.070186.000305
581 de Bono, M., & Bargmann, C. I. (1998). Natural variation in a neuropeptide Y receptor
582 homolog modifies social behavior and food response in *C. elegans*. *Cell, 94*(5), 679-
583 689. doi:10.1016/s0092-8674(00)81609-8
584 Dekker, L. V., Mcintyre, P., & Parker, P. J. (1993). Mutagenesis of the Regulatory Domain of
585 Rat Protein Kinase-C-Eta - a Molecular-Basis for Restricted Histone Kinase-Activity.
586 *Journal of Biological Chemistry, 268*(26), 19498-19504. Retrieved from <Go to
587 ISI>://WOS:A1993LW81900055
588 Dobin, A., Davis, C. A., Schlesinger, F., Drenkow, J., Zaleski, C., Jha, S., . . . Gingeras, T. R.
589 (2013). STAR: ultrafast universal RNA-seq aligner. *Bioinformatics, 29*(1), 15-21.
590 doi:10.1093/bioinformatics/bts635

591 Dokshin, G. A., Ghanta, K. S., Piscopo, K. M., & Mello, C. C. (2018). Robust Genome
592 Editing with Short Single-Stranded and Long, Partially Single-Stranded DNA Donors
593 in *Caenorhabditis elegans*. *Genetics, 210*(3), 781-787.
594 doi:10.1534/genetics.118.301532
595 Fawcett, E. M., Hoyt, J. M., Johnson, J. K., & Miller, D. L. (2015). Hypoxia disrupts
596 proteostasis in *Caenorhabditis elegans*. *Aging Cell, 14*(1), 92-101.
597 doi:10.1111/acel.12301
598 Ferkey, D. M., Sengupta, P., & L'Etoile, N. D. (2021). Chemosensory signal transduction in
599 *Caenorhabditis elegans*. *Genetics, 217*(3). doi:10.1093/genetics/iyab004
600 Ghanta, K. S., & Mello, C. C. (2020). Melting dsDNA Donor Molecules Greatly Improves
601 Precision Genome Editing in *Caenorhabditis elegans*. *Genetics, 216*(3), 643-650.
602 doi:10.1534/genetics.120.303564
603 Gourley, B. L., Parker, S. B., Jones, B. J., Zumbrennen, K. B., & Leibold, E. A. (2003).
604 Cytosolic aconitase and ferritin are regulated by iron in *Caenorhabditis elegans*. *J*
605 *Biol Chem, 278*(5), 3227-3234. doi:10.1074/jbc.M210333200
606 Gray, J. M., Karow, D. S., Lu, H., Chang, A. J., Chang, J. S., Ellis, R. E., . . . Bargmann, C. I.
607 (2004). Oxygen sensation and social feeding mediated by a *C. elegans* guanylate
608 cyclase homologue. *Nature, 430*(6997), 317-322. doi:10.1038/nature02714
609 Hallem, E. A., Spencer, W. C., McWhirter, R. D., Zeller, G., Henz, S. R., Ratsch, G., . . .
610 Ringstad, N. (2011). Receptor-type guanylate cyclase is required for carbon dioxide
611 sensation by *Caenorhabditis elegans*. *Proc Natl Acad Sci U S A, 108*(1), 254-259.
612 doi:10.1073/pnas.1017354108
613 Hallem, E. A., & Sternberg, P. W. (2008). Acute carbon dioxide avoidance in *Caenorhabditis*
614 *elegans*. *Proc Natl Acad Sci U S A, 105*(23), 8038-8043.
615 doi:10.1073/pnas.0707469105
616 Hao, Y., Yang, W., Ren, J., Hall, Q., Zhang, Y., & Kaplan, J. M. (2018). Thioredoxin shapes
617 the *C. elegans* sensory response to Pseudomonas produced nitric oxide. *Elife, 7*.
618 doi:10.7554/eLife.36833

Heiman, M. G., & Shaham, S. (2009). DEX-1 and DYF-7 establish sensory dendrite length by anchoring dendritic tips during cell migration. *Cell, 137*(2), 344-355. doi:10.1016/j.cell.2009.01.057

Hildebrandt, T. M., & Grieshaber, M. K. (2008). Three enzymatic activities catalyze the oxidation of sulfide to thiosulfate in mammalian and invertebrate mitochondria. *FEBS J, 275*(13), 3352-3361. doi:10.1111/j.1742-4658.2008.06482.x

Hiroki, S., Yoshitane, H., Mitsui, H., Sato, H., Umatani, C., Kanda, S., . . . Iino, Y. (2022). Molecular encoding and synaptic decoding of context during salt chemotaxis in *C. elegans*. *Nature Communications, 13*(1). doi:ARTN 2928 10.1038/s41467-022-30279-7

Horsman, J. W., Heinis, F. I., & Miller, D. L. (2019). A Novel Mechanism To Prevent H2S Toxicity in *Caenorhabditis elegans*. *Genetics, 213*(2), 481-490. doi:10.1534/genetics.119.302326

Jackson, M. R., Melideo, S. L., & Jorns, M. S. (2012). Human sulfide:quinone oxidoreductase catalyzes the first step in hydrogen sulfide metabolism and produces a sulfane sulfur metabolite. *Biochemistry, 51*(34), 6804-6815. doi:10.1021/bi300778t

Kaelin, W. G., Jr., & Ratcliffe, P. J. (2008). Oxygen sensing by metazoans: the central role of the HIF hydroxylase pathway. *Mol Cell, 30*(4), 393-402. doi:10.1016/j.molcel.2008.04.009

Kelley, J. L., Arias-Rodriguez, L., Patacsil Martin, D., Yee, M. C., Bustamante, C. D., & Tobler, M. (2016). Mechanisms Underlying Adaptation to Life in Hydrogen Sulfide-Rich Environments. *Mol Biol Evol, 33*(6), 1419-1434. doi:10.1093/molbev/msw020

Khan, A. A., Schuler, M. M., Prior, M. G., Yong, S., Coppock, R. W., Florence, L. Z., & Lillie, L. E. (1990). Effects of hydrogen sulfide exposure on lung mitochondrial respiratory chain enzymes in rats. *Toxicol Appl Pharmacol, 103*(3), 482-490. doi:10.1016/0041-008x(90)90321-k

645 Kim, Y. I., Cho, J. H., Yoo, O. J., & Ahnn, J. (2004). Transcriptional regulation and life-span
646 modulation of cytosolic aconitase and ferritin genes in *C.elegans*. *J Mol Biol, 342*(2),
647 421-433. doi:10.1016/j.jmb.2004.07.036
648 Kuleshov, M. V., Jones, M. R., Rouillard, A. D., Fernandez, N. F., Duan, Q. N., Wang, Z. C.,
649 . . . Ma'ayan, A. (2016). Enrichr: a comprehensive gene set enrichment analysis web
650 server 2016 update. *Nucleic Acids Research, 44*(W1), W90-W97.
651 doi:10.1093/nar/gkw377
652 Laurent, P., Soltesz, Z., Nelson, G. M., Chen, C., Arellano-Carbajal, F., Levy, E., & de Bono,
653 M. (2015). Decoding a neural circuit controlling global animal state in *C. elegans*.
654 *Elife, 4*. doi:10.7554/eLife.04241
655 Lee, S. J., Hwang, A. B., & Kenyon, C. (2010). Inhibition of Respiration Extends *C. elegans*
656 Life Span via Reactive Oxygen Species that Increase HIF-1 Activity. *Current*
657 *Biology, 20*(23), 2131-2136. doi:10.1016/j.cub.2010.10.057
658 Liao, Y., Smyth, G. K., & Shi, W. (2014). featureCounts: an efficient general purpose
659 program for assigning sequence reads to genomic features. *Bioinformatics, 30*(7),
660 923-930. doi:10.1093/bioinformatics/btt656
661 Liochev, S. I. (1996). The role of iron-sulfur clusters in in vivo hydroxyl radical production.
662 *Free Radical Research, 25*(5), 369-384. doi:Doi 10.3109/10715769609149059
663 Love, M. I., Huber, W., & Anders, S. (2014). Moderated estimation of fold change and
664 dispersion for RNA-seq data with DESeq2. *Genome Biology, 15*(12). doi:ARTN 550
665 10.1186/s13059-014-0550-8
666 Ma, D. K., Vozdek, R., Bhatla, N., & Horvitz, H. R. (2012). CYSL-1 interacts with the O2-
667 sensing hydroxylase EGL-9 to promote H2S-modulated hypoxia-induced behavioral
668 plasticity in *C. elegans*. *Neuron, 73*(5), 925-940. doi:10.1016/j.neuron.2011.12.037
669 Macosko, E. Z., Pokala, N., Feinberg, E. H., Chalasani, S. H., Butcher, R. A., Clardy, J., &
670 Bargmann, C. I. (2009). A hub-and-spoke circuit drives pheromone attraction and
671 social behaviour in *C. elegans*. *Nature, 458*(7242), 1171-1175.
672 doi:10.1038/nature07886

673 Masini, A., Salvioli, G., Cremonesi, P., Botti, B., Gallesi, D., & Ceccarelli, D. (1994). Dietary
674 Iron-Deficiency in the Rat .1. Abnormalities in Energy-Metabolism of the Hepatic
675 Tissue. *Biochimica Et Biophysica Acta-Bioenergetics, 1188*(1-2), 46-52. doi:Doi
676 10.1016/0005-2728(94)90020-5
677 Masini, A., Trenti, T., Caramazza, I., Predieri, G., Gallesi, D., & Ceccarelli, D. (1994).
678 Dietary Iron-Deficiency in the Rat .2. Recovery from Energy-Metabolism
679 Derangement of the Hepatic Tissue by Iron Therapy. *Biochimica Et Biophysica Acta-*
680 *Bioenergetics, 1188*(1-2), 53-57. doi:Doi 10.1016/0005-2728(94)90021-3
681 Mathew, N. D., Schlipalius, D. I., & Ebert, P. R. (2011). Sulfurous gases as biological
682 messengers and toxins: comparative genetics of their metabolism in model
683 organisms. *J Toxicol, 2011*, 394970. doi:10.1155/2011/394970
684 Melo, J. A., & Ruvkun, G. (2012). Inactivation of Conserved *C. elegans* Genes Engages
685 Pathogen- and Xenobiotic-Associated Defenses. *Cell, 149*(2), 452-466.
686 doi:10.1016/j.cell.2012.02.050
687 Miller, D. L., Budde, M. W., & Roth, M. B. (2011a). HIF-1 and SKN-1 Coordinate the
688 Transcriptional Response to Hydrogen Sulfide in *Caenorhabditis elegans*. *PLoS One,*
689 *6*(9). doi:ARTN e25476
690 10.1371/journal.pone.0025476
691 Miller, D. L., Budde, M. W., & Roth, M. B. (2011b). HIF-1 and SKN-1 coordinate the
692 transcriptional response to hydrogen sulfide in *Caenorhabditis elegans*. *PLoS One,*
693 *6*(9), e25476. doi:10.1371/journal.pone.0025476
694 Miller, D. L., & Roth, M. B. (2007). Hydrogen sulfide increases thermotolerance and lifespan
695 in *Caenorhabditis elegans*. *Proc Natl Acad Sci U S A, 104*(51), 20618-20622.
696 doi:10.1073/pnas.0710191104
697 Mishanina, A. V., Libiad, M., & Banerjee, R. (2015). Biogenesis of reactive sulfur species for
698 signaling by hydrogen sulfide oxidation pathways. *Nature Chemical Biology, 11*(7),
699 457-464. doi:10.1038/nchembio.1834

700 Murakami, M., Koga, M., & Ohshima, Y. (2001). DAF-7/TGF-beta expression required for
701 the normal larval development in C-elegans is controlled by a presumed guanylyl
702 cyclase DAF-11. *Mechanisms of Development, 109*(1), 27-35. doi:Doi
703 10.1016/S0925-4773(01)00507-X
704 Murayama, T., Toh, Y., Ohshima, Y., & Koga, M. (2005). The dyf-3 gene encodes a novel
705 protein required for sensory cilium formation in *Caenorhabditis elegans*. *J Mol Biol,*
706 *346*(3), 677-687. doi:10.1016/j.jmb.2004.12.005
707 Myllyharju, J., & Kivirikko, K. I. (1997). Characterization of the iron- and 2-oxoglutarate-
708 binding sites of human prolyl 4-hydroxylase. *Embo Journal, 16*(6), 1173-1180.
709 doi:DOI 10.1093/emboj/16.6.1173
710 Nicholls, P., & Kim, J. K. (1982a). Sulfide as an Inhibitor and Electron-Donor for the
711 Cytochrome-C Oxidase System. *Canadian Journal of Biochemistry, 60*(6), 613-623.
712 doi:DOI 10.1139/o82-076
713 Nicholls, P., & Kim, J. K. (1982b). Sulphide as an inhibitor and electron donor for the
714 cytochrome c oxidase system. *Can J Biochem, 60*(6), 613-623. doi:10.1139/o82-076
715 Niu, W., Lu, Z. J., Zhong, M., Sarov, M., Murray, J. I., Brdlik, C. M., . . . Reinke, V. (2011).
716 Diverse transcription factor binding features revealed by genome-wide ChIP-seq in
717 *C. elegans*. *Genome Research, 21*(2), 245-254. doi:10.1101/gr.114587.110
718 Olson, K. R., & Straub, K. D. (2016). The Role of Hydrogen Sulfide in Evolution and the
719 Evolution of Hydrogen Sulfide in Metabolism and Signaling. *Physiology (Bethesda),*
720 *31*(1), 60-72. doi:10.1152/physiol.00024.2015
721 Pekec, T., Lewandowski, J., Komur, A. A., Sobanska, D., Guo, Y., Switonska-Kurkowska,
722 K., . . . Ciosk, R. (2022). Ferritin-mediated iron detoxification promotes hypothermia
723 survival in *Caenorhabditis elegans* and murine neurons. *Nat Commun, 13*(1), 4883.
724 doi:10.1038/s41467-022-32500-z
725 Persson, A., Gross, E., Laurent, P., Busch, K. E., Bretes, H., & de Bono, M. (2009). Natural
726 variation in a neural globin tunes oxygen sensing in wild *Caenorhabditis elegans*.
727 *Nature, 458*(7241), 1030-1033. doi:10.1038/nature07820

Pfenninger, M., Lerp, H., Tobler, M., Passow, C., Kelley, J. L., Funke, E., . . . Plath, M. (2014). Parallel evolution of cox genes in H2S-tolerant fish as key adaptation to a toxic environment. *Nat Commun, 5*, 3873. doi:10.1038/ncomms4873

Philipp, T. M., Gong, W., Kohnlein, K., Ohse, V. A., Muller, F. I., Priebs, J., . . . Klotz, L. O. (2022). SEMO-1, a novel methanethiol oxidase in *Caenorhabditis elegans*, is a pro-aging factor conferring selective stress resistance. *Biofactors, 48*(3), 699-706. doi:10.1002/biof.1836

Qabazard, B., Li, L., Gruber, J., Peh, M. T., Ng, L. F., Kumar, S. D., . . . Moore, P. K. (2014). Hydrogen sulfide is an endogenous regulator of aging in *Caenorhabditis elegans*. *Antioxid Redox Signal, 20*(16), 2621-2630. doi:10.1089/ars.2013.5448

Rajan, M., Anderson, C. P., Rindler, P. M., Romney, S. J., Ferreira Dos Santos, M. C., Gertz, J., & Leibold, E. A. (2019). NHR-14 loss of function couples intestinal iron uptake with innate immunity in *C. elegans* through PQM-1 signaling. *Elife, 8*. doi:10.7554/eLife.44674

Read, A. D., Bentley, R. E. T., Archer, S. L., & Dunham-Snary, K. J. (2021). Mitochondrial iron-sulfur clusters: Structure, function, and an emerging role in vascular biology. *Redox Biology, 47*. doi:ARTN 102164

10.1016/j.redox.2021.102164

Rodriguez-Kabana, R., Jordan, J. W., & Hollis, J. P. (1965). Nematodes: Biological Control in Rice Fields: Role of Hydrogen Sulfide. *Science, 148*(3669), 524-526. doi:10.1126/science.148.3669.524

Romney, S. J., Newman, B. S., Thacker, C., & Leibold, E. A. (2011). HIF-1 regulates iron homeostasis in *Caenorhabditis elegans* by activation and inhibition of genes involved in iron uptake and storage. *PLoS Genet, 7*(12), e1002394. doi:10.1371/journal.pgen.1002394

Salvanes, A. G. V., Utne-Palm, A. C., Currie, B., & Braithwaite, V. A. (2011). Behavioural and physiological adaptations of the bearded goby, a key fish species of the extreme

environment of the northern Benguela upwelling. *Marine Ecology Progress Series, 425*, 193-202. doi:10.3354/meps08998

Semenza, G. L. (2010). Defining the role of hypoxia-inducible factor 1 in cancer biology and therapeutics. *Oncogene, 29*(5), 625-634. doi:10.1038/onc.2009.441

Shefa, U., Kim, M. S., Jeong, N. Y., & Jung, J. (2018). Antioxidant and Cell-Signaling Functions of Hydrogen Sulfide in the Central Nervous System. *Oxidative Medicine and Cellular Longevity, 2018*. doi:Artn 1873962
10.1155/2018/1873962

Siegert, I., Schodel, J., Nairz, M., Schatz, V., Dettmer, K., Dick, C., . . . Jantsch, J. (2015). Ferritin-Mediated Iron Sequestration Stabilizes Hypoxia-Inducible Factor-1 alpha upon LPS Activation in the Presence of Ample Oxygen. *Cell Reports, 13*(10), 2048-2055. doi:10.1016/j.celrep.2015.11.005

Starich, T. A., Herman, R. K., Kari, C. K., Yeh, W. H., Schackwitz, W. S., Schuyler, M. W., . . . Riddle, D. L. (1995). Mutations affecting the chemosensory neurons of *Caenorhabditis elegans*. *Genetics, 139*(1), 171-188. doi:10.1093/genetics/139.1.171

Sunda, W., Kieber, D. J., Kiene, R. P., & Huntsman, S. (2002). An antioxidant function for DMSP and DMS in marine algae. *Nature, 418*(6895), 317-320. doi:DOI 10.1038/nature00851

Swoboda, P., Adler, H. T., & Thomas, J. H. (2000). The RFX-type transcription factor DAF-19 regulates sensory neuron cilium formation in *C. elegans*. *Mol Cell, 5*(3), 411-421. doi:10.1016/s1097-2765(00)80436-0

Vora, M., Pyonteck, S. M., Popovitchenko, T., Matlack, T. L., Prashar, A., Kane, N. S., . . . Rongo, C. (2022). The hypoxia response pathway promotes PEP carboxykinase and gluconeogenesis in *C. elegans*. *Nature Communications, 13*(1). doi:ARTN 6168
10.1038/s41467-022-33849-x

Walter, P. B., Knutson, M. D., Paler-Martinez, A., Lee, S., Xu, Y., Viteri, F. E., & Ames, B. N. (2002). Iron deficiency and iron excess damage mitochondria and mitochondrial

782 DNA in rats. *Proceedings of the National Academy of Sciences of the United States of*
783 *America, 99*(4), 2264-2269. doi:DOI 10.1073/pnas.261708798
784 Xu, X. M., & Moller, S. G. (2011). Iron-Sulfur Clusters: Biogenesis, Molecular Mechanisms,
785 and Their Functional Significance. *Antioxidants & Redox Signaling, 15*(1), 271-307.
786 doi:10.1089/ars.2010.3259
787 Zhao, L., Fenk, L. A., Nilsson, L., Amin-Wetzel, N. P., Ramirez-Suarez, N. J., de Bono, M.,
788 & Chen, C. (2022). ROS and cGMP signaling modulate persistent escape from
789 hypoxia in *Caenorhabditis elegans*. *PLoS Biol, 20*(6), e3001684.
790 doi:10.1371/journal.pbio.3001684
791 Zimmer, M., Gray, J. M., Pokala, N., Chang, A. J., Karow, D. S., Marletta, M. A., . . .
792 Bargmann, C. I. (2009). Neurons detect increases and decreases in oxygen levels
793 using distinct guanylate cyclases. *Neuron, 61*(6), 865-879.
794 doi:10.1016/j.neuron.2009.02.013
795
796
797 **Figure legends**
798 **Figure 1. cGMP signaling in ASJ neurons contributes to H_2S avoidance**
799 (**A–H**) Locomotory responses to a switch from 7% O_2 to 150 ppm H_2S balanced with 7% O_2
800 for animals of the indicated genotype: WT (N2) and *daf-19(m86)* (**A**); WT and *dyf-3(m185)*
801 (**B**); WT and *dyf-7(m539)* (**C**); WT, *daf-11(m47)* and *tax-4(p678)* (**D**); WT and *tax-2(p691)*
802 (**E**); WT, *daf-2(e1370), daf-16(mgDf47) and daf-2(e1370); daf-16(mgDf47) double mutants*
803 (**F**); WT, *daf-7(e1372), daf-3(mgDf90) and daf-7(e1372); daf-3(mgDf90) double mutants*
804 (**G**); WT and *gcy-9(tm7632)* (**H**). In this and subsequent figures for H_2S assay, red bars on the
805 x-axis represent two intervals (4–5 minutes and 11–12 minutes, labeled as a and b
806 respectively in Figure 1D, F, G, J and K) used for statistical analysis unless otherwise
807 indicated. **** = $p < 0.0001$, *** = $p < 0.001$, ** = $p < 0.01$, * = $p < 0.05$, ns = not
808 significant, Mann–Whitney U test. (**I**) Comparison between the acute locomotory response of
809 WT animals to 150 ppm H_2S balanced with 7% O_2 and the acute locomotory response to 5%

810 CO_2 balanced with 7% O_2. Red bars on the x-axis indicate two intervals (3-4 minutes and 11-
811 12 minutes) used for statistical analysis. * = $p < 0.05$, ns = not significant, Mann–Whitney U
812 test. (**J**) Locomotory responses to a switch from 7% O_2 to 150 ppm H_2S balanced with 7% O_2
813 for animals of the indicated genotype: WT, *daf-11(m47)* and transgenic *daf-11(m47)*
814 expressing *daf-11* genomic DNA in ASJ neurons (two independent lines). *** = $p < 0.001$, **
815 = $p < 0.01$, * = $p < 0.05$, Mann–Whitney U test. (**K**) Locomotory responses to a switch from
816 7% O_2 to 150 ppm H_2S balanced with 7% O_2 for animals of the indicated genotype: WT, *tax-*
817 *4(p678)* and transgenic *tax-4(p678)* expressing *tax-4* cDNA in ASJ neurons (two independent
818 lines). *** = $p < 0.001$, ** = $p < 0.01$, * = $p < 0.05$, Mann–Whitney U test.
819
820 **Figure 2. Activation of O_2 sensing circuit antagonizes H_2S avoidance**
821 (**A**) Locomotory responses to a switch from 7% O_2 to 150 ppm H_2S balanced with 7% O_2 for
822 WT animals, wild isolates CB4858 and CB4855. Red bars on the x-axis represent two
823 intervals (4–5 minutes and 11–12 minutes, labeled as a and b respectively), used for statistical
824 analyses. ** = $p < 0.01$, * = $p < 0.05$, Mann–Whitney U test. (**B, C**) Locomotory responses to
825 a switch from 7% O_2 to 150 ppm H_2S balanced with 7% O_2 for animals of the indicated
826 genotype: WT and *npr-1(ad609)* (**B**); WT, *npr-1(ad609) and* transgenic *npr-1(ad609)*
827 expressing *npr-1* in RMG neurons using Cre-LoxP system (Macosko et al., 2009) (**C**). Red
828 bars on the x-axis indicate two intervals (4-5 minutes and 11-12 minutes) used for statistical
829 analysis. **** = $p < 0.0001$, *** = $p < 0.001$, ** = $p < 0.01$, Mann–Whitney U test. (**D–G**)
830 Locomotory responses to a switch from 7% O_2 to 150 ppm H_2S balanced with 7% O_2 for
831 animals of the indicated genotype: WT, *npr-1(ad609), gcy-35(ok769)* and *npr-1(ad609); gcy-*
832 *35(ok769)* double mutants (**D**); WT, *npr-1(ad609), tax-4(p678)* and *npr-1(ad609); tax-*
833 *4(p678)* double mutants (**E**); WT, *npr-1(ad609), qaIs2241*(genetic ablation of AQR, PQR and
834 URX neurons) and *npr-1(ad609); qaIs 2241* (**F**); WT, *npr-1(ad609), npr-1(ad609); gcy-*
835 *35(ok769)* double mutants and *transgenic npr-1(ad609); gcy-35(ok769)* double mutants
836 expressing *gcy-35* cDNA under *gcy-37* promoter, which drives expression in O_2 sensing
837 neurons (**G**). Red bars on the x-axis indicate two intervals (4-5 minutes and 11-12 minutes)

838 used for statistical analysis. *** = $p < 0.001$, ** = $p < 0.01$, * = $p < 0.05$, ns = not significant,
839 Mann–Whitney U test.
840
841 **Figure 3. Prolonged H_2S exposure reprograms gene expression in *C. elegans***
842 (**A**) Venn diagram displaying the number of differentially expressed genes after 1-hour
843 exposure to 50 ppm or 150 ppm H_2S balanced with 7% O_2 in WT animals. p<1e-10. (**B**) Venn
844 diagram displaying the number of differentially expressed genes after 1-hour, 2-hour and 12-
845 hour exposure to 150 ppm H_2S balanced with 7% O_2 in WT animals. p<1e-10. (**C, D**)
846 Significantly enriched GO categories for differentially expressed genes with adjusted p value
847 <1e-10 in WT animals exposed to 50 ppm (**C**) or 150 ppm (**D**) H_2S balanced with 7% O_2 for 1
848 hour. (**E, F**) Volcano plots showing the differentially expressed genes with adjusted p value
849 <1e-10 in WT animals exposed to 50 ppm (**E**) or 150 ppm (**F**) H_2S balanced with 7% O_2 for 1
850 hour. A set of genes involved in H_2S detoxification, cysteine metabolism and stress response
851 were highlighted in red.
852
853 **Figure 4. Acute response to H_2S is modulated by HIF-1 signaling**
854 (**A–D**) Locomotory responses to a switch from 7% O_2 to 150 ppm H_2S balanced with 7% O_2
855 for animals of the indicated genotype: WT and *hif-1(ia4)* (**A**); WT, *egl-9(sa307) and vhl-*
856 *1(ok161)* (**B**); WT, *egl-9(sa307), hif-1(ia4) and egl-9(sa307); hif-1(ia4)* double mutants (**C**);
857 WT, *vhl-1(ok161), hif-1(ia4) and vhl-1(ok161); hif-1(ia4)* double mutants (**D**). Red bars on
858 the x-axis represent two intervals (4–5 minutes and 11–12 minutes, labeled as a and b
859 respectively), used for statistical analyses. *** = $p < 0.001$, ** = $p < 0.01$, * = $p < 0.05$, ns =
860 not significant, Mann–Whitney U test. (**E**) Locomotory responses of WT animals to a switch
861 from 7% O_2 to 150 ppm H_2S balanced with 7% O_2 after 0, 12, 24 or 36 hours in 1% O_2. Red
862 bars on the x-axis represent two intervals (4–5 minutes and 11–12 minutes, labeled as a and b
863 respectively), used for statistical analyses. *** = $p < 0.001$, ** = $p < 0.01$, ns = not
864 significant, Mann–Whitney U test. (**F**) Locomotory responses to a switch from 7% O_2 to 150
865 ppm H_2S balanced with 7% O_2 for animals carrying the non-degradable form of HIF-1. Non-

866 degradable form of HIF-1 (P621A and P621G) are expressed from a pan-neuronal promoter
867 *unc-14* or form *hif-1* endogenous promoter, respectively. Red bars on the x-axis represent two
868 intervals (4–5 minutes and 11–12 minutes, labeled as a and b respectively), used for statistical
869 analyses. ** = $p < 0.01$, ns = not significant, Mann–Whitney U test. (**G–J**) Locomotory
870 responses to a switch from 7% O_2 to 150 ppm H_2S balanced with 7% O_2 for animals of the
871 indicated genotype: WT and *sqrd-1(tm3378)* (**G**); WT and *ethe-1(yum2895)* (**H**); WT, *cysl-*
872 *1(ok762), cysl-2(ok3516)* and *cysl-3(yum4)* (**I**); WT and *semo-1(yum2889)* (**J**). Red bars on
873 the x-axis represent two intervals (4–5 minutes and 11–12 minutes, labeled as a and b
874 respectively), used for statistical analyses. *** = $p < 0.001$, ** = $p < 0.01$, * = $p < 0.05$, ns =
875 not significant, Mann–Whitney U test.
876
877 **Figure 5. Labile iron pool is critical to sustain the locomotory activity in H_2S**
878 (**A, B**) Volcano plots showing the relative expression of the genes involved in the regulation
879 of iron homeostasis in WT animals after 2-hour exposure with 50 ppm (**A**) or 150 ppm (**B**)
880 H_2S balanced with 7% O_2. (**C**) Locomotory responses to a switch from 7% O_2 to 150 ppm
881 H_2S balanced with 7% O_2 for WT animals, WT animals pretreated with 100 μM 2,2′-
882 Bipyridyl (BP) and WT animals pretreated with 5 mg/ml ferric ammonium citrate (FAC) in
883 the presence of food for 16 hours. Red bars on the x-axis represent two intervals (4–5 minutes
884 and 14–15 minutes, labeled as a and b respectively), used for statistical analyses. ** = $p <$
885 0.01, * = $p < 0.05$, ns = not significant, Mann–Whitney U test. (**D**) Locomotory responses to a
886 switch from 7% O_2 to 150 ppm H_2S balanced with 7% O_2 for animals of the indicated
887 genotype: WT, *smf-3(ok1305)* and *ftn-1(ok3625).* Red bars on the x-axis represent two
888 intervals (4–5 minutes and 14–15 minutes, labeled as a and b respectively), used for statistical
889 analysis. *** = $p < 0.001$, * = $p < 0.05$, ns = not significant, Mann–Whitney U test. (**E**)
890 Locomotory responses to a switch from 7% O_2 to 150 ppm H_2S balanced with 7% O_2 for WT
891 animals and animals overexpressing *ftn-1* genomic DNA under its own promoter (#1 and #2
892 indicate two independent lines). Red bars on the x-axis represent two intervals (4–5 minutes
893 and 11–12 minutes, labeled as a and b respectively), used for statistical analysis. **** = $p <$

894 0.0001, ** = $p < 0.01$, ns = not significant, Mann–Whitney U test. (**F, G**) Locomotory
895 responses to a switch from 7% O_2 to 150 ppm H_2S balanced with 7% O_2 for animals of the
896 indicated genotype: WT, *hif-1(ia4)* and *hif-1(ia4)* mutants pretreated with 5 mg/ml ferric
897 ammonium citrate (FAC) for 16 hours (**F**)*;* WT, *hif-1(ia4), ftn-1(ok3625)* and *hif-1(ia4); ftn-*
898 *1(ok3625)* double mutants (**G**). Red bars on the x-axis represent two intervals (4–5 minutes
899 and 8–9 minutes) used for statistical analysis. * = $p < 0.05$, ns = not significant, Mann–
900 Whitney U test.
901
902 **Figure 6. Mitochondrial function is required for acute response to H_2S**
903 (**A–D**) Locomotory responses to a switch from 7% O_2 to 150 ppm H_2S balanced with 7% O_2
904 for animals of the indicated genotype: WT and *gas-1(fc21)* (**A**); WT and *clk-1(qm30)* (**B**);
905 WT and *mev-1(kn1)* (**C**); WT and *isp-1(qm150)* (**D**). Red bars on the x-axis represent two
906 intervals (4–5 minutes and 11–12 minutes) used for statistical analysis. **** = $p < 0.0001$, **
907 = $p < 0.01$, * = $p < 0.05$, Mann–Whitney U test. (**E**) Locomotory responses to a switch from
908 7% O_2 to 150 ppm H_2S balanced with 7% O_2 for WT animals pretreated with 10 μM rotenone
909 for 0 minute, 10 minutes, 30 minutes, 60 minutes or 120 minutes. Red bars on the x-axis
910 represent two intervals (4–5 minutes and 11–12 minutes, labeled as a and b respectively),
911 used for statistical analysis. *** = $p < 0.001$, ** = $p < 0.01$, * = $p < 0.05$, ns = not significant,
912 Mann–Whitney U test.
913
914 **Figure 1—figure supplement 1. Acute locomotory responses of *C. elegans* to hydrogen**
915 **sulfide.**
916 (**A**) Changes in the locomotory activity of WT animals evoked by a switch from 7% O_2 to 150
917 ppm H_2S balanced with 7% O_2. (**B**) Reorientation movements (omega turns) of WT animals
918 evoked by a switch from 7% O_2 to 150 ppm H_2S balanced with 7% O_2. (**C**) Changes in
919 reversal frequency in WT animals experiencing a switch from 7% O_2 to 150 ppm H_2S
920 balanced with 7% O_2. (**D**) Locomotory activity of WT was recorded for 2 minutes at 7%

921 O_2 and 148 minutes at 150 ppm H_2S balanced with 7% O_2 followed by 2 additional minutes at
922 7% O_2. (**E**) Locomotory activity of WT animals evoked by acute hypoxia after preincubation
923 for 148 minutes at 150 ppm H_2S balanced with 7% O_2. Locomotory activity was recorded for
924 2 minutes at each gas interval. (**F**) Locomotory responses of WT animals to different
925 concentrations of H_2S balanced with 7% O_2. Red bars on the x-axis represent two intervals
926 (4–5 minutes and 11–12 minutes, labeled as a and b respectively) used for statistical analysis.
927 **** = $p < 0.0001$, ** = $p < 0.01$, * = $p < 0.05$, ns = not significant, Mann–Whitney U test.
928

929 **Figure 1—figure supplement 2. Acute response to H_2S is regulated by multiple signaling**
930 **pathways**

931 (**A–E**) Locomotory responses to a switch from 7% O_2 to 150 ppm H_2S balanced with 7% O_2
932 for animals of the indicated genotype: WT and *tax-6(ok2065)* (**A**); WT and *cnb-1(ok276)* (**B**);
933 WT and *nhr-49(nr2041)* (**C**); WT animals and WT animals starved for 24 hours (**D**); WT and
934 *daf-2(e1370)* (**E**). To assay *daf-2* animals, WT and *daf-2* mutants were kept in 15°C. L4
935 animals were picked, maintained at 25°C until day-one adults and assayed at room
936 temperature. Red bars on the x-axis represent two intervals (4–5 minutes and 11–12 minutes),
937 used for statistical analysis. **** = $p < 0.0001$, *** = $p < 0.001$, ** = $p < 0.01$, ns = not
938 significant, Mann–Whitney U test. (**F–I**) Locomotory responses to a switch from 7% O_2 to
939 150 ppm H_2S balanced with 7% O_2 for animals of the indicated genotype: WT, *daf-11(m47)*
940 and transgenic *daf-11* mutants expressing *daf-11* genomic DNA in different subsets of
941 neurons (**F–H**); The detailed expression pattern of each promoter is listed in (**I**). Red bars on
942 the x-axis represent two intervals (4–5 minutes and 11–12 minutes, labeled as a and b
943 respectively), used for statistical analysis. * = $p < 0.05$, ns = not significant, Mann–Whitney
944 U test.
945

946 **Figure 2—figure supplement 1. NPR-1 signaling modulates locomotory response to H_2S**

947 (**A**) Locomotory responses to a switch from 7% O_2 to 150 ppm H_2S balanced with 7% O_2 for
948 WT animals and wild isolate CB4856. Red bars on the x-axis represent two intervals (4–5
949 minutes and 11–12 minutes), used for statistical analysis. ** = $p < 0.01$, ns = not significant,
950 Mann–Whitney U test. (**B**) Optogenetic stimulation of RMG neurons using
951 channelrhodopsin-2 (ChR2). Expressing ChR2 in RMG neurons were achieved using Cre-
952 LoxP system (Macosko et al., 2009). L4 animals were picked, grown for 16 hours on the
953 seeded plates containing ATR, and assayed as day-one adults. Blue light was delivered
954 throughout the assay. Red bars on the x-axis represent two intervals (4–5 minutes and 11–12
955 minutes), used for statistical analysis. ** = $p < 0.01$, ns = not significant, Mann–Whitney U
956 test. (**C**) Activation of O_2 sensing neurons by expressing a gain-of-function allele of *pkc-1*
957 under *gcy-37* promoter. Red bars on the x-axis represent two intervals (4–5 minutes and 11–
958 12 minutes), used for statistical analysis. * = $p < 0.05$, ns = not significant, Mann–Whitney U
959 test.
960
961 **Figure 3—figure supplement 1. Transcriptome reprogramming induced by H_2S**
962 **exposure**
963 (**A**) Venn diagram displaying the number of differentially expressed genes after exposure in
964 50 ppm H_2S balanced with 7% O_2 in WT animals for 1 hour, 2 hours or 12 hours. Adjusted *p*
965 value <1e-10. (**B, C**) Significantly enriched GO categories for differentially expressed genes
966 with adjusted *p* value <1e-10 in WT animals exposed to 50 ppm (**B**) or 150 ppm (**C**) H_2S
967 balanced with 7% O_2 for 2 hours. (**D, E**) Volcano plot showing the differentially expressed
968 genes with adjusted *p* value <1e-10 in WT animals exposed to 50 ppm (**D**) or 150 ppm (**E**)
969 H_2S balanced with 7% O_2 for 2 hours. A set of genes involved in H_2S detoxification, cysteine
970 metabolism and stress response were highlighted in red. (**F, G**) The number of HIF-1(**F**) and
971 SKN-1(**G**) target genes induced by 50 ppm or 150 ppm H_2S exposure for 1hour, 2 hours or 12
972 hours in WT animals, with Adjusted *p* value < 1e-30. (**H–J**) Venn diagrams displaying the
973 number of differentially expressed genes (adjusted *p* value <1e-10) in WT animals of the
974 indicated conditions: animals were exposed to 50 ppm or 150 ppm H_2S for 1hour (**H**); for

975 2hours (**I**); and for 12 hours (**J**). (**K, L**) Volcano plots showing the differentially expressed
976 genes (adjusted *p* value <1e-10) in WT animals that were exposed to either 50 ppm (**K**) or
977 150 ppm (**L**) H_2S balanced with 7% O_2 for 12 hours. A set of genes involved in H_2S
978 detoxification, cysteine metabolism and stress response were highlighted in red.
979
980 **Figure 5—figure supplement 1. *ftn-1* expression is consistently repressed in H_2S**
981 (**A–D**) Volcano plots showing the relative expression of the genes involved in the regulation
982 of iron homeostasis (*ftn-1*, *ftn-2* and *smf-3*) in WT animals of the indicated conditions: 1-hour
983 exposure in 50 ppm H_2S balanced with 7% O_2 (**A**); 1-hour exposure in 150 ppm H_2S balanced
984 with 7% O_2 (**B**); 12-hour exposure in 50 ppm H_2S balanced with 7% O_2 (**C**); and 12-hour
985 exposure in 150 ppm H_2S balanced with 7% O_2 (**D**). (**E, F**) Locomotory responses to a switch
986 to 7% to 1% O_2 for animals of the indicated treatments or genotypes: WT animals, WT
987 animals treated with 100 μM 2,2′-Bipyridyl (BP), and WT animals treated with 5 mg/ml ferric
988 ammonium citrate (FAC) for 16 hours (**E**); WT and WT animals overexpressing *ftn-1*
989 genomic DNA under its own promoter (#1 and #2 indicate two independent lines) (**F**). Red
990 bar on the x-axis represents time interval (3–4 minutes) used for statistical analysis. * = $p <$
991 0.05, ns = not significant, Mann–Whitney U test.

Figure 1

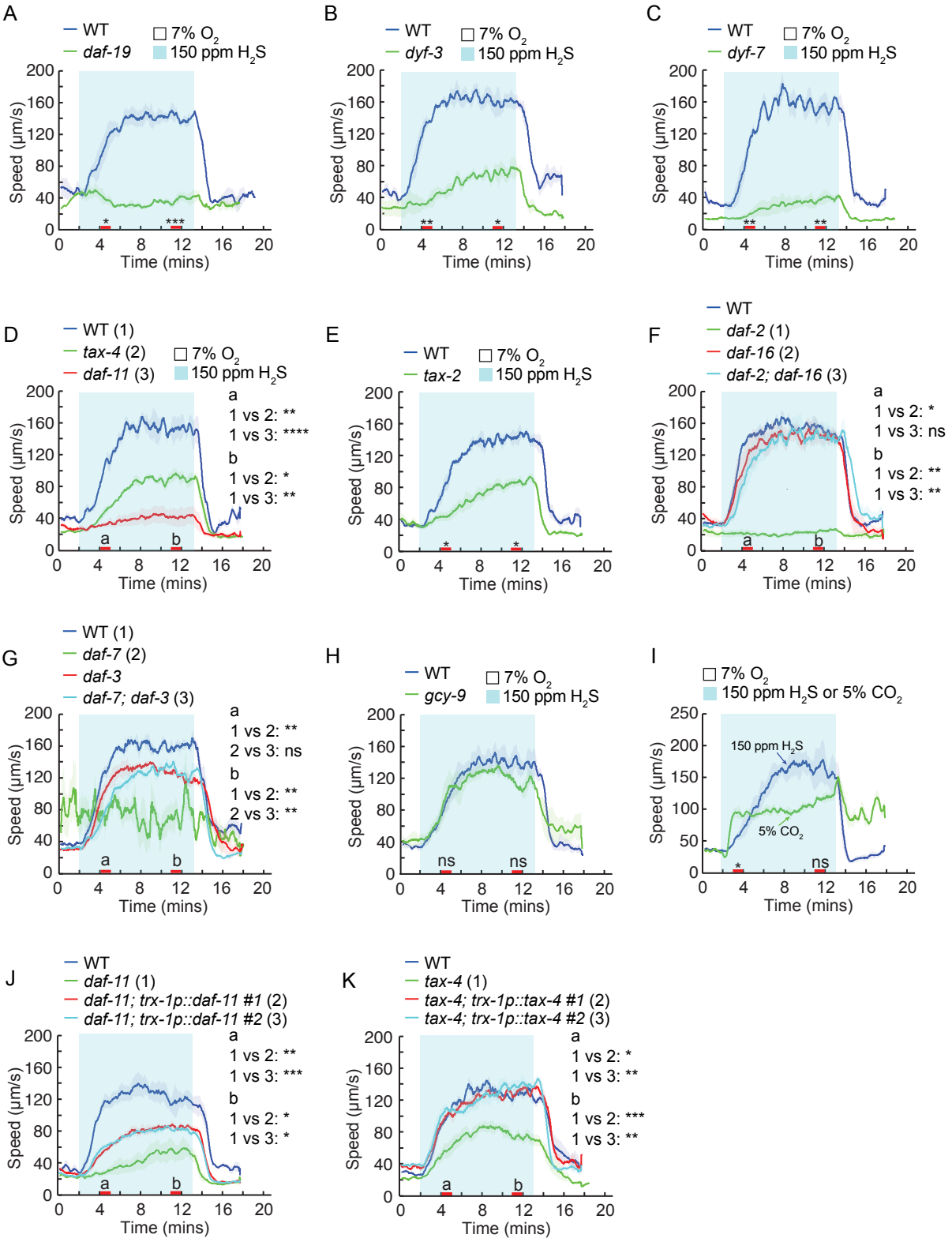
A
WT
daf-19
7% O2
150 ppm H2S
Speed (µm/s)
Time (mins)
B
WT
dyf-3
7% O2
150 ppm H2S
C
WT
dyf-7
7% O2
150 ppm H2S
D
WT (1)
tax-4 (2)
daf-11 (3)
7% O2
150 ppm H2S
a
1 vs 2: **
1 vs 3: ****
b
1 vs 2: *
1 vs 3: **
E
WT
tax-2
7% O2
150 ppm H2S
F
WT
daf-2 (1)
daf-16 (2)
daf-2; daf-16 (3)
a
1 vs 2: *
1 vs 3: ns
b
1 vs 2: **
1 vs 3: **
G
WT (1)
daf-7 (2)
daf-3
daf-7; daf-3 (3)
a
1 vs 2: **
2 vs 3: ns
b
1 vs 2: **
2 vs 3: **
H
WT
gcy-9
7% O2
150 ppm H2S
ns
I
7% O2
150 ppm H2S or 5% CO2
150 ppm H2S
5% CO2
J
WT
daf-11 (1)
daf-11; trx-1p::daf-11 #1 (2)
daf-11; trx-1p::daf-11 #2 (3)
a
1 vs 2: **
1 vs 3: ***
b
1 vs 2: *
1 vs 3: *
K
WT
tax-4 (1)
tax-4; trx-1p::tax-4 #1 (2)
tax-4; trx-1p::tax-4 #2 (3)
a
1 vs 2: *
1 vs 3: **
b
1 vs 2: ***
1 vs 3: **

Figure 2

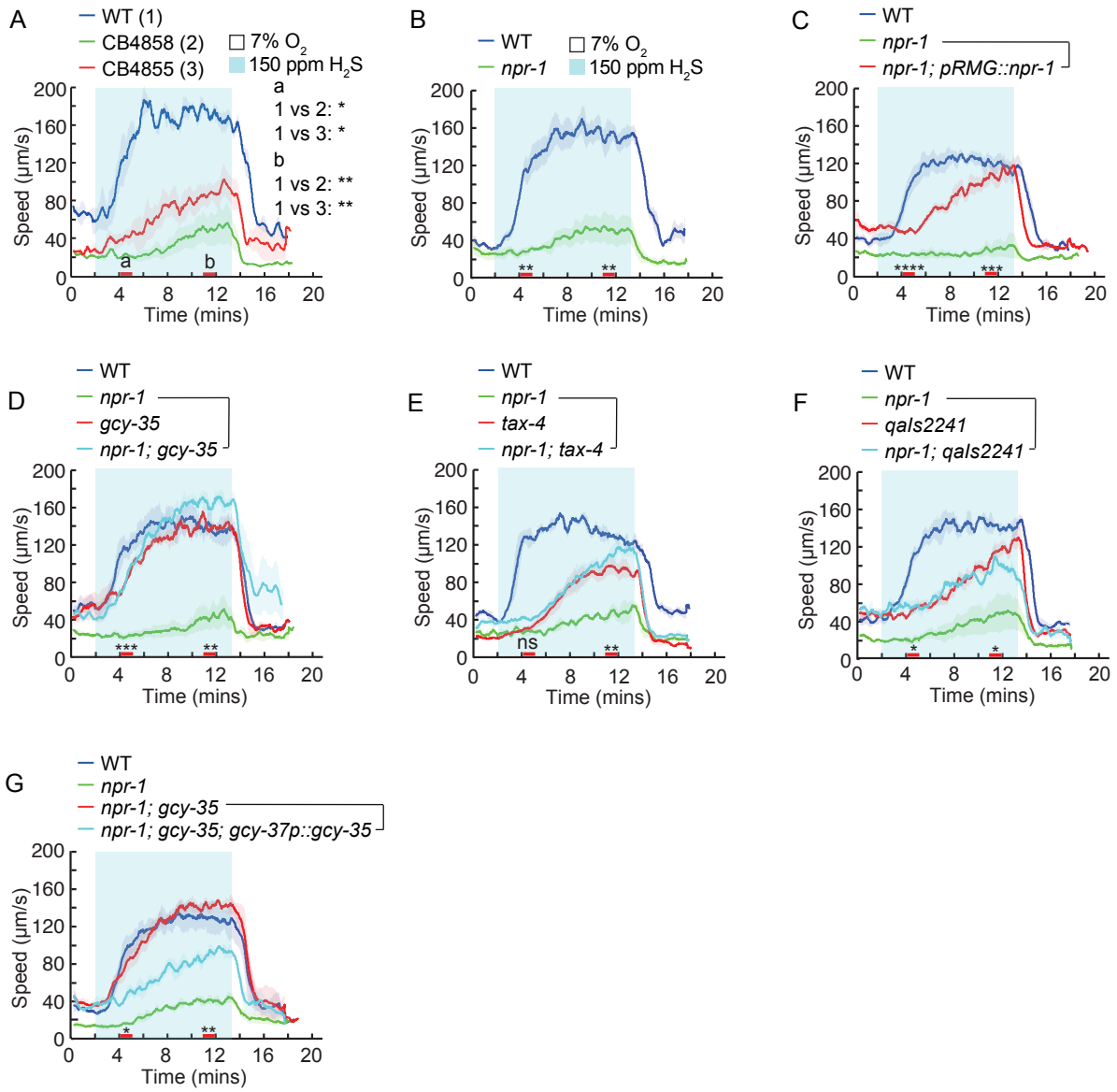
A
WT (1)
CB4858 (2)
CB4855 (3)
7% O2
150 ppm H2S
a
1 vs 2: *
1 vs 3: *
b
1 vs 2: **
1 vs 3: **
Speed (µm/s)
Time (mins)
B
WT
npr-1
7% O2
150 ppm H2S
C
WT
npr-1
npr-1; pRMG::npr-1
D
WT
npr-1
gcy-35
npr-1; gcy-35
E
WT
npr-1
tax-4
npr-1; tax-4
ns
F
WT
npr-1
qals2241
npr-1; qals2241
G
WT
npr-1
npr-1; gcy-35
npr-1; gcy-35; gcy-37p::gcy-35

Figure 3

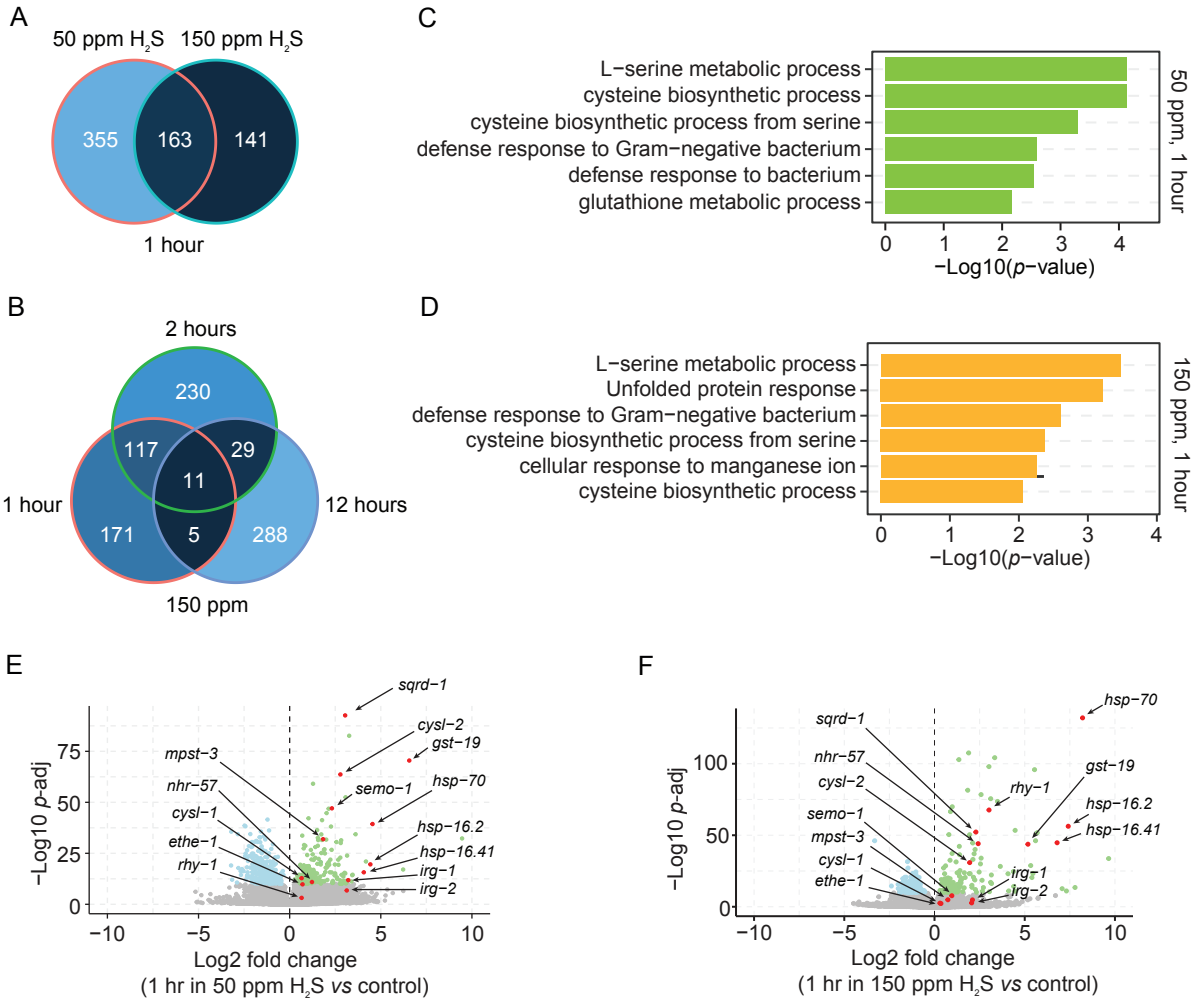
A
50 ppm H2S
150 ppm H2S
355
163
141
1 hour
B
2 hours
230
117
29
11
1 hour
12 hours
171
5
288
150 ppm
C
L−serine metabolic process
cysteine biosynthetic process
cysteine biosynthetic process from serine
defense response to Gram−negative bacterium
defense response to bacterium
glutathione metabolic process
0
1
2
3
4
−Log10(p−value)
50 ppm, 1 hour
D
L−serine metabolic process
Unfolded protein response
defense response to Gram−negative bacterium
cysteine biosynthetic process from serine
cellular response to manganese ion
cysteine biosynthetic process
0
1
2
3
4
−Log10(p−value)
150 ppm, 1 hour
E
sqrd−1
cysl−2
gst−19
mpst−3
nhr−57
semo−1
hsp−70
cysl−1
ethe−1
hsp−16.2
hsp−16.41
rhy−1
irg−1
irg−2
−Log10 p-adj
75
50
25
0
−10
−5
0
5
10
Log2 fold change
(1 hr in 50 ppm H2S vs control)
F
hsp−70
sqrd−1
nhr−57
gst−19
cysl−2
rhy−1
hsp−16.2
semo−1
hsp−16.41
mpst−3
cysl−1
irg−1
ethe−1
irg−2
−Log10 p-adj
100
50
0
−10
−5
0
5
10
Log2 fold change
(1 hr in 150 ppm H2S vs control)

Figure 4

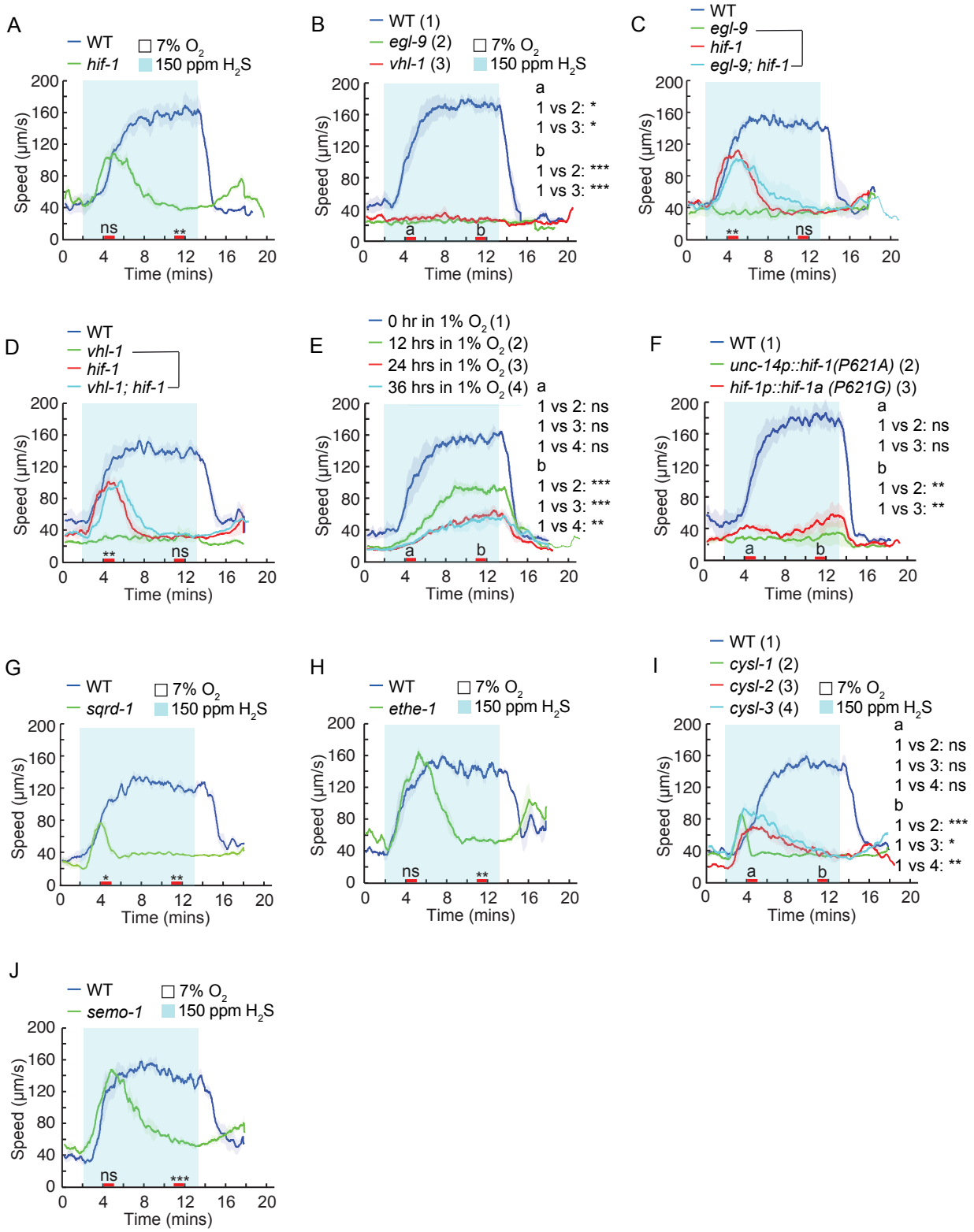
A
WT
hif-1
7% O2
150 ppm H2S
Speed (µm/s)
Time (mins)
ns
**
B
WT (1)
egl-9 (2)
vhl-1 (3)
7% O2
150 ppm H2S
a
1 vs 2: *
1 vs 3: *
b
1 vs 2: ***
1 vs 3: ***
C
WT
egl-9
hif-1
egl-9; hif-1
**
ns
D
WT
vhl-1
hif-1
vhl-1; hif-1
**
ns
E
0 hr in 1% O2 (1)
12 hrs in 1% O2 (2)
24 hrs in 1% O2 (3)
36 hrs in 1% O2 (4)
a
1 vs 2: ns
1 vs 3: ns
1 vs 4: ns
b
1 vs 2: ***
1 vs 3: ***
1 vs 4: **
F
WT (1)
unc-14p::hif-1(P621A) (2)
hif-1p::hif-1a (P621G) (3)
a
1 vs 2: ns
1 vs 3: ns
b
1 vs 2: **
1 vs 3: **
G
WT
sqrd-1
7% O2
150 ppm H2S
*
**
H
WT
ethe-1
7% O2
150 ppm H2S
ns
**
I
WT (1)
cysl-1 (2)
cysl-2 (3)
cysl-3 (4)
7% O2
150 ppm H2S
a
1 vs 2: ns
1 vs 3: ns
1 vs 4: ns
b
1 vs 2: ***
1 vs 3: *
1 vs 4: **
J
WT
semo-1
7% O2
150 ppm H2S
ns
***

Figure 5

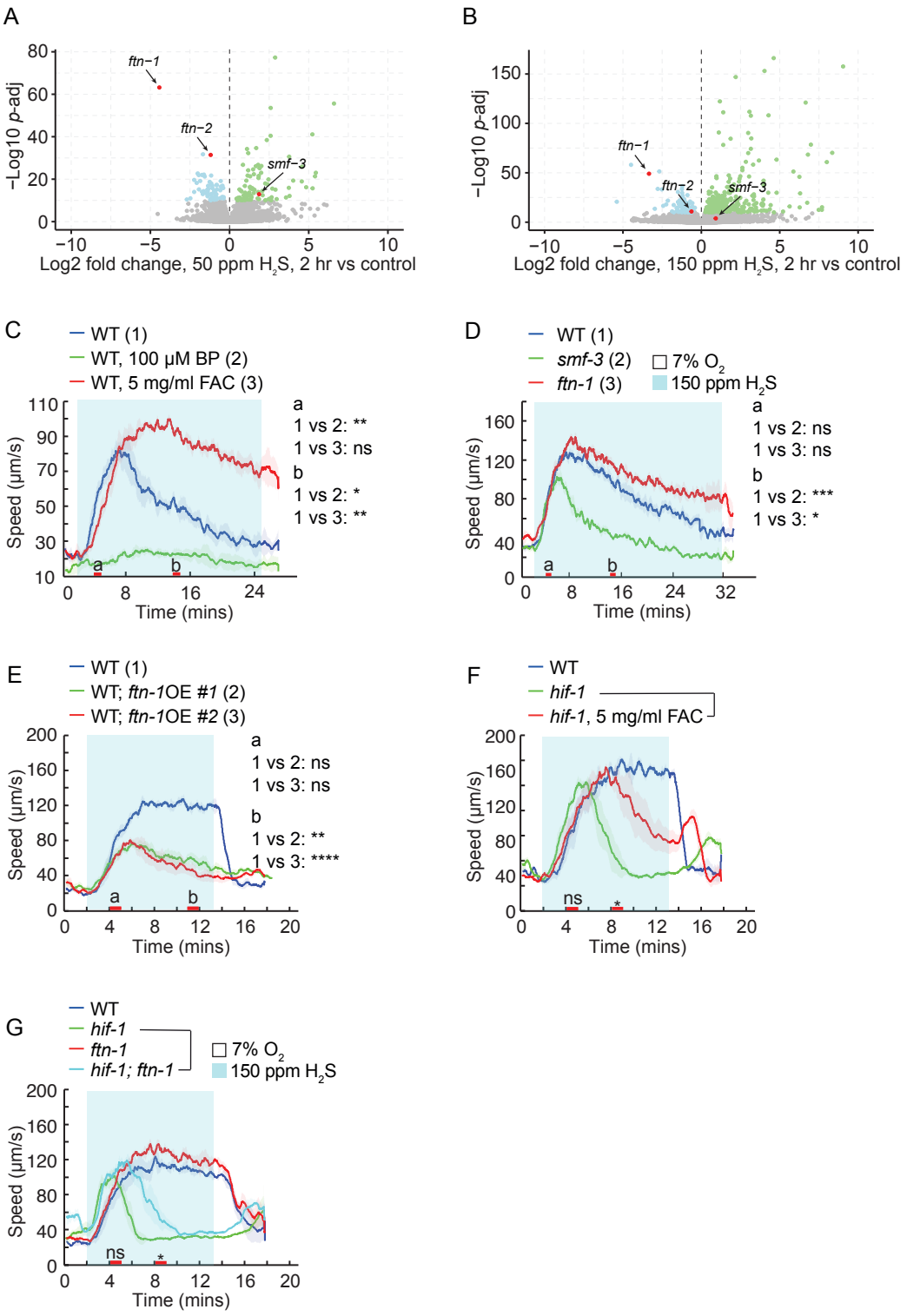
A
−Log10 p-adj
ftn−1
ftn−2
smf−3
Log2 fold change, 50 ppm H2S, 2 hr vs control
B
−Log10 p-adj
ftn−1
ftn−2
smf−3
Log2 fold change, 150 ppm H2S, 2 hr vs control
C
WT (1)
WT, 100 μM BP (2)
WT, 5 mg/ml FAC (3)
a
1 vs 2: **
1 vs 3: ns
b
1 vs 2: *
1 vs 3: **
Speed (μm/s)
Time (mins)
D
WT (1)
smf-3 (2)
ftn-1 (3)
7% O2
150 ppm H2S
a
1 vs 2: ns
1 vs 3: ns
b
1 vs 2: ***
1 vs 3: *
Speed (μm/s)
Time (mins)
E
WT (1)
WT; ftn-1OE #1 (2)
WT; ftn-1OE #2 (3)
a
1 vs 2: ns
1 vs 3: ns
b
1 vs 2: **
1 vs 3: ****
Speed (μm/s)
Time (mins)
F
WT
hif-1
hif-1, 5 mg/ml FAC
ns
*
Speed (μm/s)
Time (mins)
G
WT
hif-1
ftn-1
hif-1; ftn-1
7% O2
150 ppm H2S
ns
*
Speed (μm/s)
Time (mins)

Figure 6

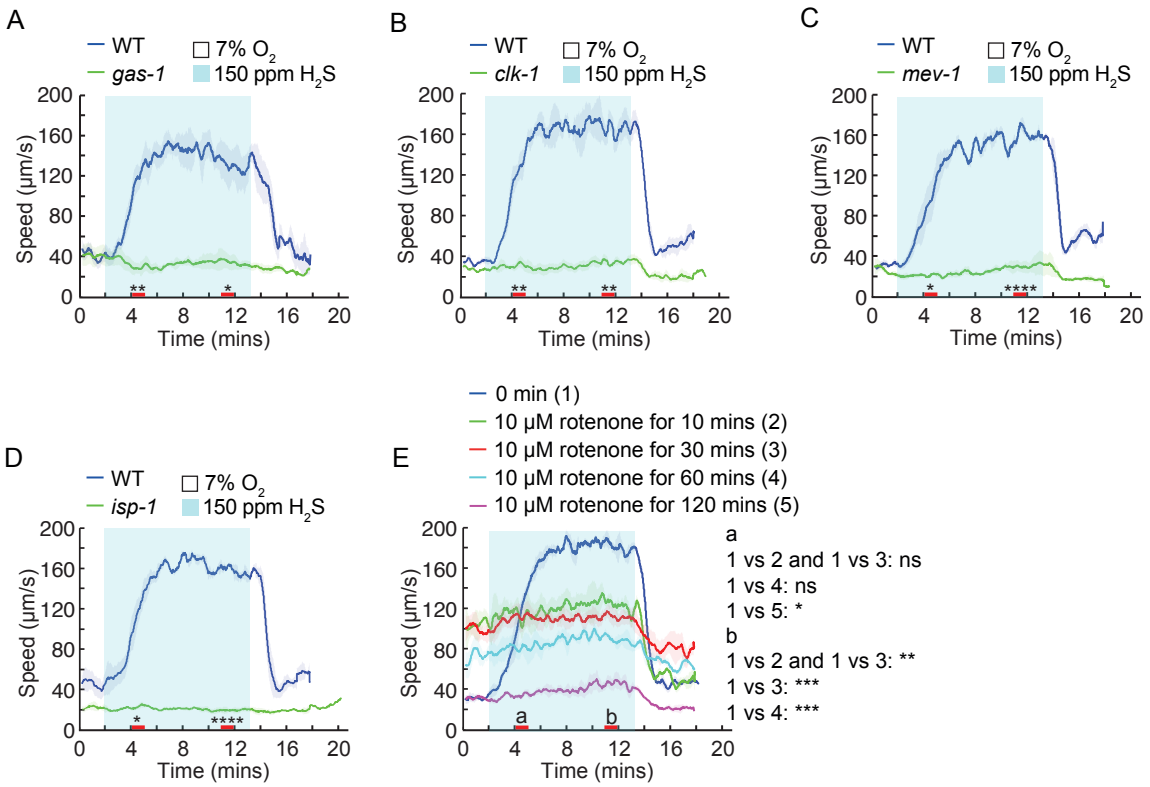
A
WT
gas-1
7% O2
150 ppm H2S
Speed (µm/s)
Time (mins)
B
WT
clk-1
7% O2
150 ppm H2S
Speed (µm/s)
Time (mins)
C
WT
mev-1
7% O2
150 ppm H2S
Speed (µm/s)
Time (mins)
D
WT
isp-1
7% O2
150 ppm H2S
Speed (µm/s)
Time (mins)
E
0 min (1)
10 µM rotenone for 10 mins (2)
10 µM rotenone for 30 mins (3)
10 µM rotenone for 60 mins (4)
10 µM rotenone for 120 mins (5)
Speed (µm/s)
Time (mins)
a
1 vs 2 and 1 vs 3: ns
1 vs 4: ns
1 vs 5: *
b
1 vs 2 and 1 vs 3: **
1 vs 3: ***
1 vs 4: ***

Figure 1-figure supplement 1

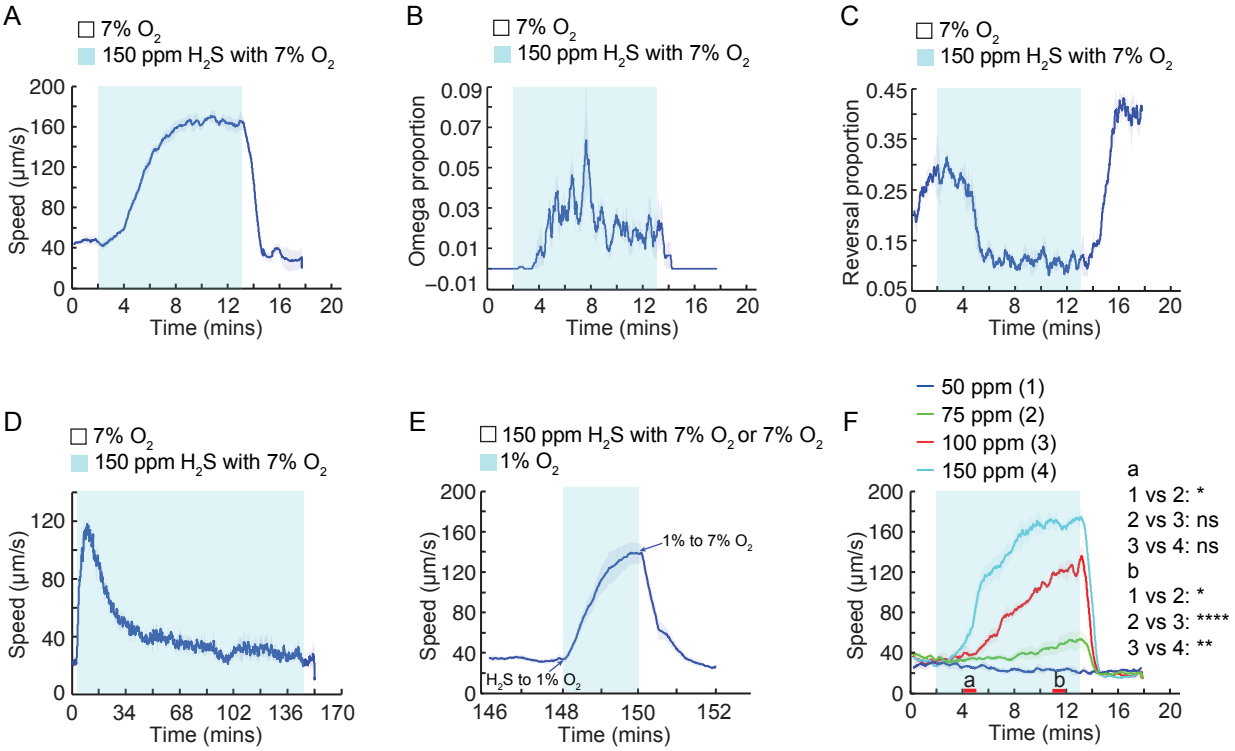

Figure 1-figure supplement 2

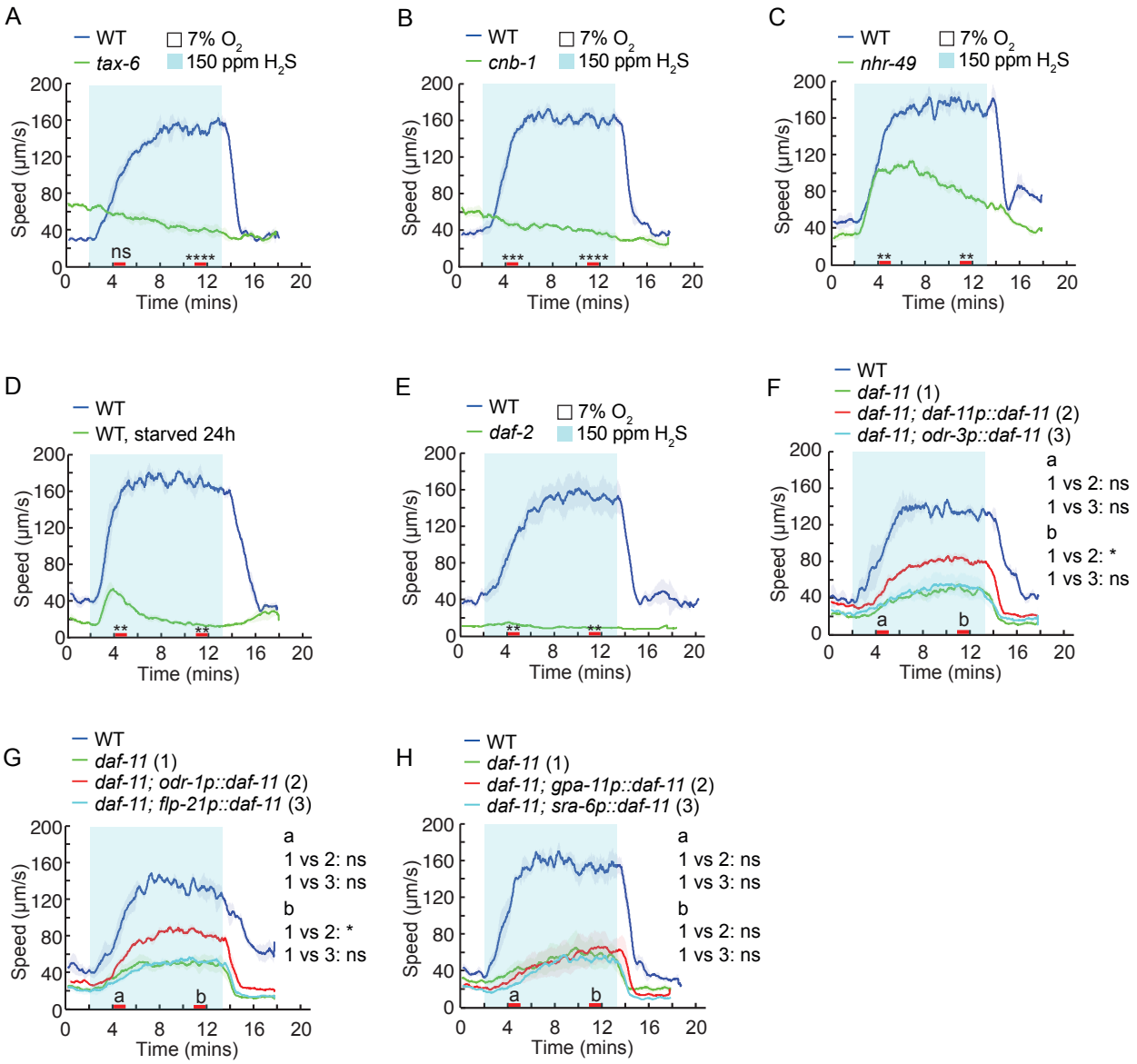

I

Promoter	neurons																
Pdaf-11	ASH	AWB	AWC	ASJ	ASK	ADL	ASI	ASE									
Podr-3	ASH	AWB	AWC						ADF	AWA							
Podr-1		AWB	AWC	ASJ	ASK		ASI										
Pflp-21	ASH					ADL	ASI	ASE			FLP	URA	RMG	MC	M2	M4	
Pgpa-11	ASH					ADL											
Psra-6	ASH						ASI										PVQ

Figure 2-figure supplement 1

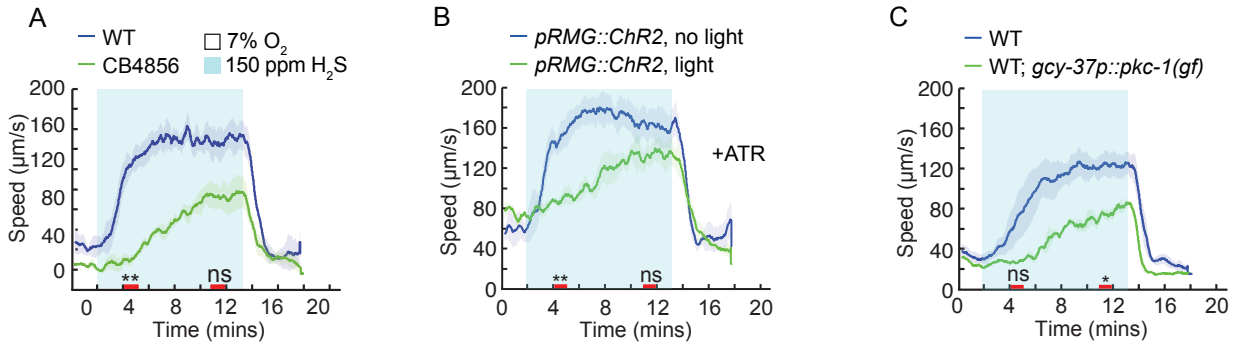

Figure 3-figure supplement 1

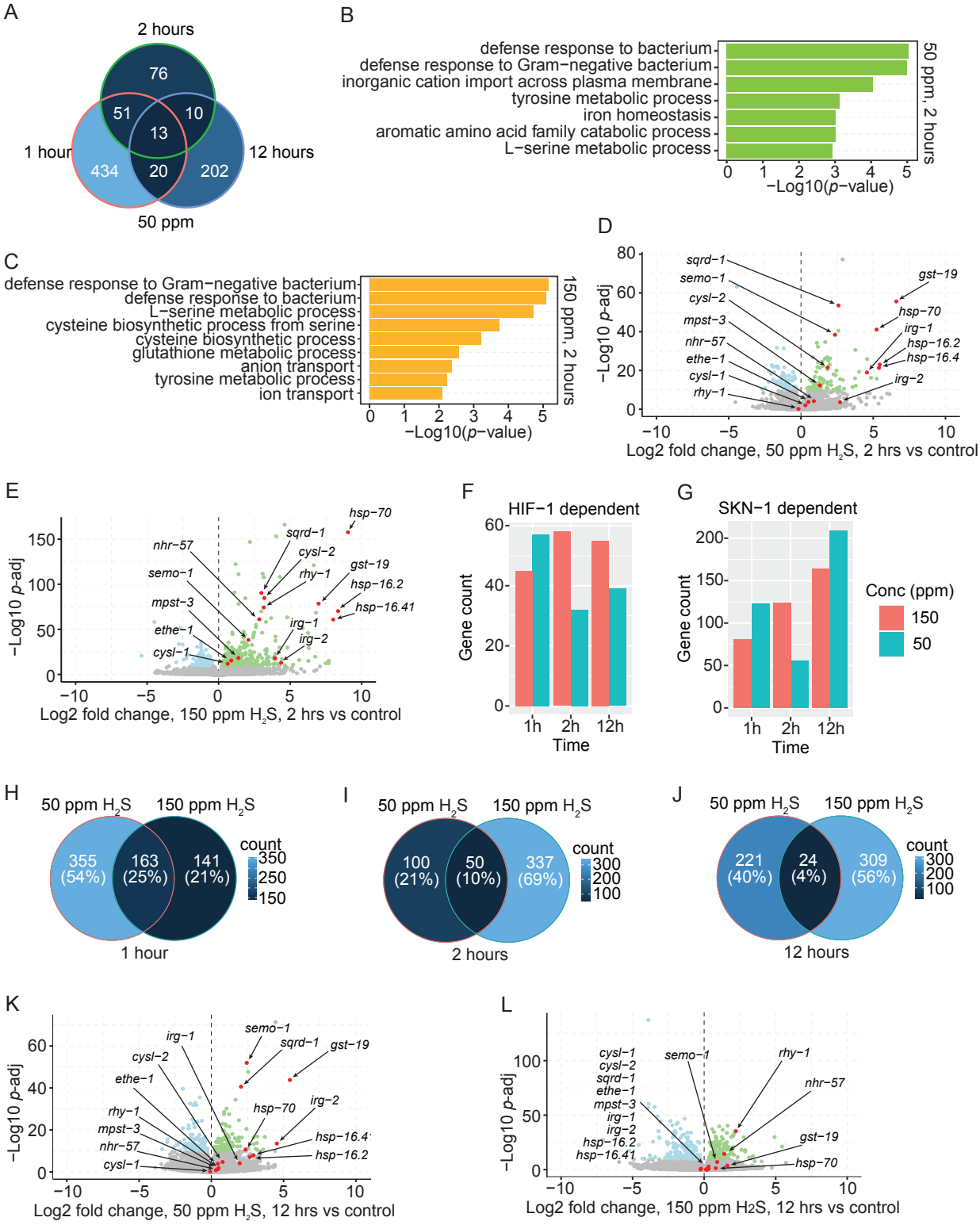
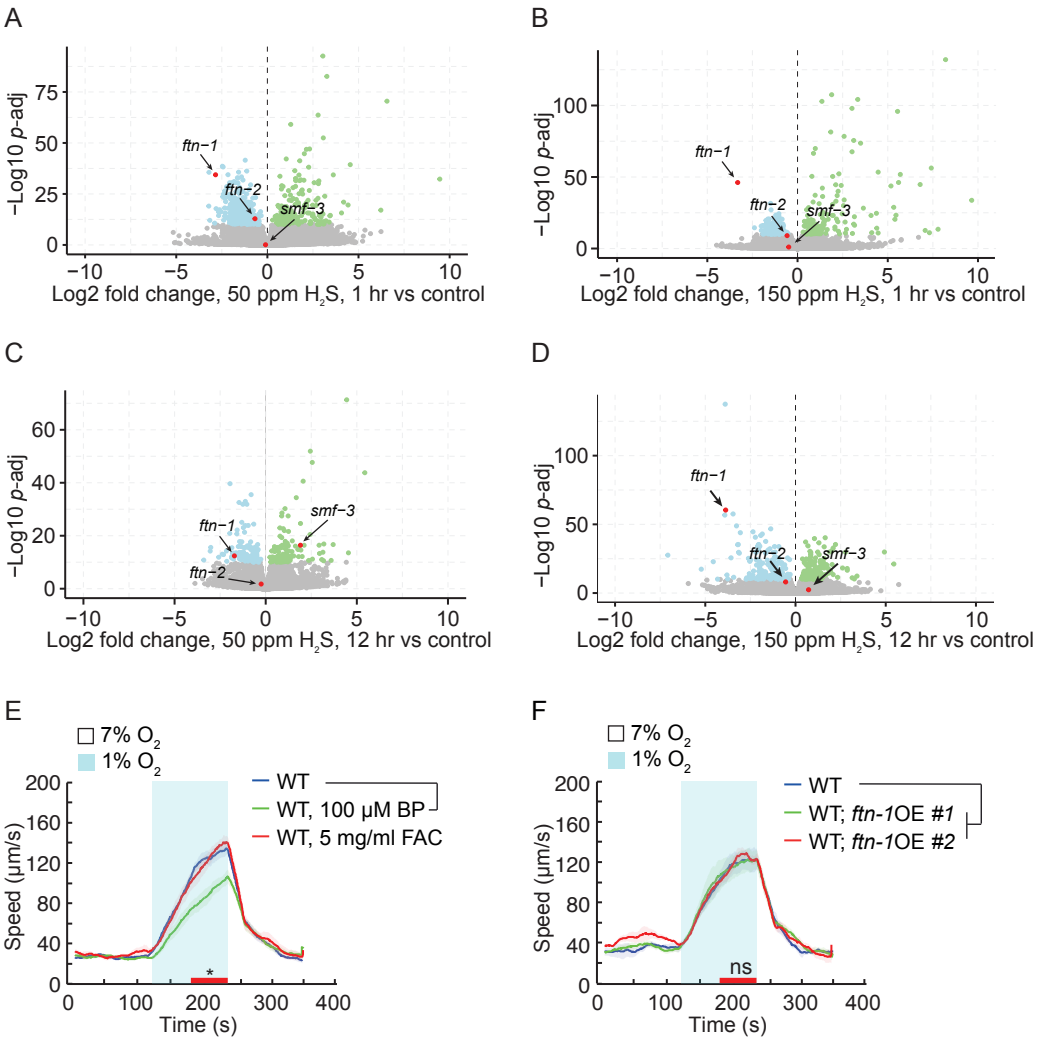
Figure 5-figure supplement 1